SAPIENZA
UNIVERSITÀ DI ROMA

Dottorato di Ricerca in Scienze Botaniche

XXVI ciclo

STRUCTURAL AND FUNCTIONAL STUDY OF PROTEINS INVOLVED IN THE ACCUMULATION AND PERCEPTION OF OLIGOGALACTURONIDES

Federico Andreani

Once more into the fray.
Into the last good fight I'll ever know.
Live and die on this day.
Live and die on this day.

John Ottway

Docente Guida
Prof. Felice Cervone

Coordinatore Dottorato di Ricerca in Scienze Botaniche
Prof. ssa Maria Maddalena Altamura

Commissione giudicatrice

Prof. ssa Alessandra Cona
Università degli Studi Roma Tre

Prof. ssa Antonella Canini
Università degli Studi di Roma "Tor Vergata"

Prof. Claudio Caprari
Università degli Studi del Molise

INDEX

1. INTRODUCTION

1.1 Plant Immunity

In an environment full of harmful microbes, an efficient sensing of danger and a rapid mounting of defense responses are crucial for the survival of plants as well as of animals (Bent, A. F. and Mackey, D. 2007). Protective mechanisms, collectively referred to as immunity, include the perception of conserved pathogen- or microbe-associated molecular patterns (PAMPs or MAMPs) by germ line-encoded pattern recognition receptors (PRRs) (Chisholm, S. T. et al. 2006). In plants, the activation upon PAMP recognition of a complex array of defense responses that eventually terminates microbial infection (Boller, T. and Felix, G. 2009) has been indicated as PAMP-triggered immunity (PTI) (Zipfel, C. 2009). Successful pathogens need to suppress PTI to express their full virulence potential, and do so by using effectors or toxins leading to the so-called effector-triggered susceptibility (ETS). Many plants then evolve the ability to sense specific pathogen effectors through the so-called resistance (R)-proteins and mount a second level of defense called effector-triggered immunity (ETI) (Gassmann, W. and Bhattacharjee, S. 2012). ETI leads to a defense response that is stronger than PTI and normally accompanied by a form of programmed cell death called hypersensitive response (Nimchuk, Z. et al. 2003). Like in animals, plant immunity also relies on the ability to sense invading microbes by means of endogenous molecular

patterns that are released only when the tissue is infected or damaged (damage-associated molecular patterns or DAMPs) (De Lorenzo et al., 2011). In these cases, it is the discrimination between self and altered self that leads to the activation of the immune system (fig. 1).

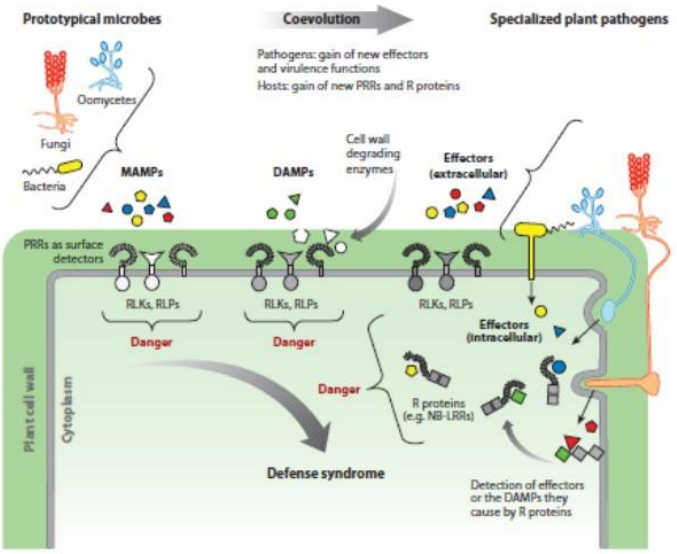

Figure 1. Schematic representation of the perception of Microbe-associated molecular patterns (MAMPs), damage-associated molecular patterns (DAMPs) Extracellular MAMPs of prototypical microbes and DAMPs released by their enzymes are recognized through pattern recognition receptors (PRRs). In the course of coevolution, pathogens gain effectors as virulence factors, and plants evolve new PRRs and resistance (R) proteins to perceive the effectors. When MAMPs, DAMPs, and effectors are recognized by PRRs and R proteins, a stereotypical defense syndrome is induced. RLK, receptor-like kinase; RLP, receptor-like protein; NB-LRR, nucleotide binding-site–leucine-rich repeat (Adapted from Boller and Felix, 2009).

The ability to perceive and process information via cell surface receptors is a basic property of living systems and often involves

receptors characterized by the presence of a ligand-binding extracellular domain (ectodomain), a single membrane spanning domain and a cytoplasmic kinase domain (RK) (Osakabe, Y. et al. 2013). In plants, a high number (more than 400 in Arabidopsis) of receptors with the typical transmembrane RK structure (RLKs, receptor-like kinases) are grouped in different families (Gou, X. et al. 2010, Shiu, S. H. and Bleecker, A. B. 2001a). This class of receptors is structurally defined by the presence of a ligand-binding extracellular domain, a single membrane-spanning domain and a cytoplasmic tyrosine kinase domain. In plants, receptor-like kinases (RLKs) are a class of transmembrane kinases similar in basic structure to the RTKs (Walker, J. C. 1994). In Arabidopsis alone, it has been reported that there are more than 300 RLKs (McCarty, D. R. and Chory, J. 2000). Plant RLKs can be distinguished from animal RTKs by the finding that all RLKs examined to date show serine/threonine kinase specificity, whereas animal receptor kinases, with the exception of transforming growth factor-β (TGF-β) receptors, are tyrosine kinases. In the Arabidopsis genome there are 620 sequences related to RLKs (Shiu, S. H. and Bleecker, A. B. 2001a). Ten of these sequences showed greatest sequence similarity to the Raf kinase family. For the remaining 610 Arabidopsis sequences, 193 did not have an obvious receptor configuration as determined by the absence of putative signal sequences and/or

transmembrane regions. The other 417 genes with receptor configurations can be classified into more than 21 structural classes by their extracellular domains. Recognition domains of RLKs include different scaffolds such as LysM domains, epidermal growth factor (EGF)-like repeats or leucine- rich repeat (LRR) motifs (Gou, X. et al. 2010, Shiu, S. H. and Bleecker, A. B. 2001a). LRR-RLKs represent the largest number of RLKs with more than 220 members (Shiu, S. H. and Bleecker, A. B. 2001b), comprises the PRRs for bacterial proteinaceous PAMPs, FLS2 (FLAGELLINE SENSITIVE 2) and EFR (EF-Tu receptor) (Boller, T. and Felix, G. 2009). LRR domains are known from crystallographic studies to form a highly ordered horseshoe-like solenoid structure, with a structural backbone consisting of an α-helix and connecting residues on the outer, convex side of the horseshoe and a β-strand/β-turn with sequence LxxLxLxxN on the inner, concave side, where the solvent exposed residues x are thought to be involved in ligand binding (Bent, A. F. and Mackey, D. 2007, Kajava, A. V. and Kobe, B. 2002).

FLS2 is characterized by 28 LRR modules and perceives flagellin via the minimal epitope flg22, leading to callose formation, accumulation of defense proteins, production of reactive oxygen species (ROS) and activation of mitogen-activated protein kinases (MAPKs) accompanied by inhibition of seedling growth (Felix, G. et al. 1999). Responsiveness to flg22 is shared by members of all major

groups of higher plants, indicating that the PRR for this epitope of bacterial flagellin is evolutionarily ancient (Boller, T. and Felix, G. 2009)(Boller and Felix 2009) (fig. 2).

The regulatory RLK BRI1-ASSOCIATED KINASE1 (BAK1) forms a flg22-induced complex with FLS2 within seconds and functions very early in flg22-response pathways because BAK1 is required for all known downstream flg22- signaling responses (Chinchilla, D. et al. 2007a, Chinchilla, D. et al. 2009, Heese, A. et al. 2007, Ntoukakis, V. et al. 2011, Smith, J. M. et al. 2013). FLS2 is one of only a few plant RLKs shown to undergo ligand-induced endocytosis and subsequent degradation (Choi, S. W. et al. 2013, Goehre, V. et al. 2008, Lu, D. et al. 2011, Robatzek, S. et al. 2006). As determined by live-cell imaging, treatment with active flg22 (derived from *Pseudomonas syringae*) results in internalization and subsequent degradation of ectopically expressed FLS2 tagged with green fluorescent protein (FLS2-GFP) within 60 min post-elicitation (Robatzek, S. et al. 2006). In contrast, elicitation with inactive flg22 (*Agrobacterium tumefaciens*) had no effect (Robatzek, S. et al. 2006). Very recent quantitative live-cell imaging studies further show that when ectopically expressed in *Arabidopsis thaliana* and *Nicotiana benthamiana*, FLS2-GFP traffics through early, late and multi-vesicular endosomes in response to flg22 (Beck, M. et al. 2012, Choi, S. W. et al. 2013). Recently it has been demonstrated

that FLS2 undergoes ligand- induced degradation in a ligand-, time- and dose-dependent manner: this ligand-induced degradation of FLS2 plays a role in desensitizing host cells to the stimulus and is likely required for receptor turnover from the cell surface (Smith, J. M. et al. 2013).

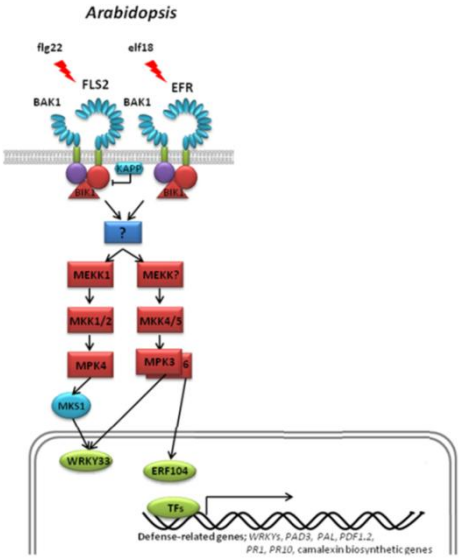

Figure 2. Models forpatternrecognitionreceptor-mediated phosphorylation pathwaysin *Arabidopsis*

FLS2 and BAK1 associate with the membrane-associated cytoplasmic kinase *Botrytis*-induced kinase1 (BIK1) *in vitro* and *in vivo* (Lu *et al*.,2010). In the resting state, *Arabidopsis* FLS2 interacts with BIK1. Flg22 perception induces FLS2 and BAK1 association and phosphorylation. Activated BAK1 phosphorylates BIK1, which in turn transphosphorylates the FLS2/BAK1 complex. Phosphorylated BIK1 is released from the FLS2/BAK1 complex to activate downstream intracellular signaling. At least two MAPK cascades are initiated downstream of activated FLS2, leading to the phosphorylation of the adaptor protein MKS1 and the transcription factors, AtWRKY33 and ERF104. Kinase-associated protein phosphatase (KAPP), a PP2C, blocks the activated FLS2 signaling and attenuates the downstream

immuneresponse. EFR-mediated immunity is believed to trigger the same MAPK cascadesas FLS2.

The EFR protein has a similar structure to FLS2 and also belongs to the RLK family LRR-RK XII, but contains 21 LRRs instead of 28 (Shiu, S. H. and Bleecker, A. B. 2003). Within this family, six genes, including EFR, are closely related with respect to the kinase domain. Its MAMP activity was assigned to its N terminus: Peptides corresponding to the acetylated N terminus of EF-Tu, called elf18 and elf26, triggered MAMP responses in Arabidopsis at subnanomolar concentrations (Kunze, G. et al. 2004). Responsiveness to elf18/elf26 was found in various Brassicaceae species but not in members of other plant families tested, indicating that perception of EF-Tu as a MAMP is an innovation in the Brassicaceae (Kunze, G. et al. 2004). The elicitor activity of bacterial EF-Tu was discovered serendipitously as well: In control experiments with boiled extracts from an *Escherichia coli flic*-mutant lacking flagellin, an additional protein with strong elicitor activity was detected and identified as the elongation factor EF-Tu, one of the most abundant and most conserved proteins of bacteria (Kunze, G. et al. 2004). Its MAMP activity was assigned to its N terminus, corresponding to the acetylated N terminus of EF-Tu, called elf18 and elf26, triggered MAMP responses in Arabidopsis at subnanomolar concentrations (Zipfel, C. et al. 2006) (fig.2).

Response to endogenous signals originating from stressed or injured cells, the so-called “regulation from within,” is now emerging as an important function of the immune system. Endogenous molecules with elicitor activity are released from cellular components during pathogen attack or abiotic stresses, and have been indicated as damage-associated molecular patterns (DAMPs) in both plants (Boller, T. and Felix, G. 2009, De Lorenzo, G. et al. 2011, Galletti, R. et al. 2009, Ranf, S. et al. 2011) and animals, where they have also been called alarmins (Bianchi, M. E. 2007, Jiang, D. et al. 2011, Lotze, M. T. et al. 2007b).

The structural barrier represented by the plant cell wall may be breached by pathogen-secreted lytic enzymes or mechanical damage and generate molecules that function as endogenous elicitors or DAMPs. Plant cell walls are composed by high molecular weight polysaccharides, highly glycosylated proteins and lignin (Somerville, C. et al. 2004). DAMPs typically appear in the apoplast (cell wall) and, similarly to MAMPs, serve as danger signals to activate the immune response (Lotze, M. T. et al. 2007a). A 18-amino-acid peptide called systemin has the typical features of DAMPs. In tomato plants, systemin, triggers a defense response similar to that induced by mechanical wounding (Schilmiller, A. L. and Howe, G. A. 2005). Because its precursor prosystemin is a cytoplasmic protein, systemin is expected to be released only upon cell injury and to act as a

DAMP in the neighbouring cells. The systemin's receptors are not yet been identified (Hind, S. R. et al. 2010). Another example of DAMP is the 23-amino-acid peptide AtPep1: this was isolated from Arabidopsis leaves as a molecule that induces alkalinisation in Arabidopsis cell cultures at subnanomolar concentrations and amplifies the responses triggered by PAMPs (Huffaker, A. and Ryan, C. A. 2007). AtPep1 is the C-terminal part of a small, putatively cytoplasmic protein encoded by PROPEP1, a gene induced by wounding, methyl jasmonate, ethylene, flg22 and AtPep1 (Krol, E. et al. 2010). Constitutive overexpression of the PROPEP1 gene causes an increased resistance against Pythium (Huffaker, A. and Ryan, C. A. 2007). PEPR1, the receptor of AtPep1, belongs to the LRR-RLK family XI; double mutants defective in PEPR1 and its homolog PEPR2 fail to respond to AtPep1, AtPep2 and AtPep3 (Krol, E. et al. 2010).

Enzymes that breach the plant cell wall (cell wall-degrading enzymes: CWDEs) are produced by many pathogens and are essential components of their offensive arsenal (Jung, S. K. et al. 2012). CWDEs have been shown to be important for fungal pathogens that lack specialised penetration structures and for necrotrophic pathogens (Lagaert, S. et al. 2009). The most extensively studied CWDEs are the endopolygalacturonases (PGs; EC 3.2.1.5), which cleave the linkages between α-1,4 D-galacturonic

acid residues in non-methylated homogalacturonan (HGA), the major component of pectin (Garcia-Maceira, F. I. et al. 2001). PGs are well-known virulence factors of phytopathogenic fungi and some isoforms have been shown to be necessary for pathogenicity of *Botrytis cinerea*, *Sclerotinia sclerotiorum*, and other fungal species (Kars, I. et al. 2005, Zuppini, A. et al. 2005). PGs cause cell separation, tissue maceration and release of mono- di- and three-saccharides utilized as carbon source for the pathogen growth (De Lorenzo, G. et al. 2001). To counteract the fungal invasion, plants localize in the apoplast the Polygalacturonase Inhibitor Protein (PGIP); by inhibiting the action of PGs, PGIPs not only hinder pectin degradation, but also favor the accumulation of elicitor-active oligogalacturonides (OGs) (De Lorenzo, G. et al. 1994, De Lorenzo, G. et al. 2001, De Lorenzo, G. and Ferrari, S. 2002). OGs with a degree of polymerization (DP) between 10 and 15 are biologically active in triggering defense response (Cote, F. and Hahn, M. G. 1994). This size is optimal for the formation of Ca^{2+}-mediated intermolecular cross-links resulting in structures called “eggboxes” (Braccini, I. and Perez, S. 2001, Cabrera, J. C. et al. 2008), that are thought to be necessary for OG activity. Modification of the reducing end of OGs does not affect the formation of egg boxes (Cabrera, J. C. et al. 2008) and does not affect elicitor activity (Ferrari, S. et al. 2013) (fig 3).

A wide range of defense responses are elicited by OGs, in several plant species, including accumulation of phytoalexins (Davis, D. A. and Currier, W. W. 1986), glucanase, and chitinase (Broekaert, W. F. and Peumans, W. J. 1988, Davis, G. L. and Hunter, E. 1987), deposition of callose, production of reactive oxygen species (ROS; (Bellincampi, D. et al. 2000, Galletti, R. et al. 2008), and nitric oxide (Rasul, S. et al. 2012). Notably, the responses triggered by OGs in Arabidopsis largely overlap those activated by MAMPs. For instance, transcript profiling of seedlings treated with either OGs or flg22, indicated an extensive overlap of responses, at least at the early times after treatment (30-60 min) (Denoux, C. et al. 2008).

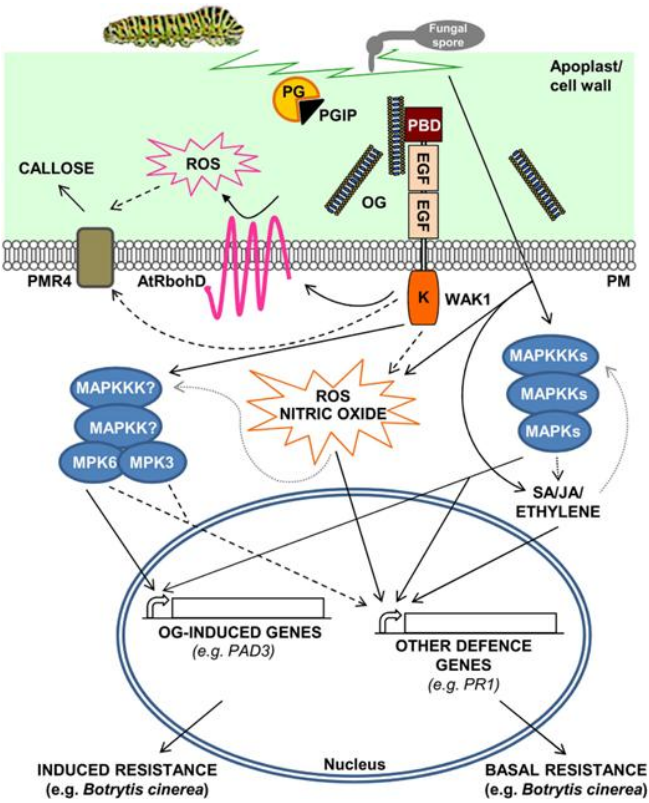

Figure 3. A model for the activation of *Arabidopsis thaliana* defense responses triggered by oligogalacturonides (OGs).

OGs are released from the cell wall after degradation of homogalacturonan by mechanical damage or by the action of hydrolytic enzymes such as PGs, secreted by pathogens. PGIPs in the apoplast modulate PG activity, favoring the accumulation of elicitor-active OGs. OGs are perceived by WAK1 and trigger defense responses such as ROS accumulation through the activation of the NADPH oxidase AtRbohD, nitricoxide production, callose deposition, and MAPK-mediated activation of defense gene expression. (Adapted from Ferrari *et al.*, 2013).

Furthermore, both OGs and flg22 trigger a robust oxidative burst mediated by the nicotinamide adenine dinucleotide phosphate (NADPH) oxidase AtRbohD, which is at least partially responsible for the subsequent production of callose (Galletti, R. et al. 2008, Zhang, X. et al. 2007). O_2^--generating NADPH oxidases are the major producers of ROS during the oxidative burst triggered by pathogens or elicitors (Torres, M. A. et al. 2006b). In Arabidopsis, the NADPH oxidase AtrbohD, which is required for the production of ROS during infection with different bacterial and fungal pathogens (Torres, M. A. et al. 2006a), is required also for OG-induced accumulation of H_2O_2 (Galletti, R. et al. 2008).

Arabidopsis leaves treated with OGs, are protected against infection with *Botrytis cinerea*, suggesting that production of these elicitors at the site of infection contributes to activate defense responses (Aziz, A. et al. 2004, Ferrari, S. et al. 2007). Protection against *B. cinerea* induced by OGs, like protection against *P. syringae* induced by flg22 (Chinchilla, D. et al. 2007b), occurs both in wild type Arabidopsis and in mutants impaired in salicylic acid (SA)-, jasmonate (JA)-, or ethylene (ET)- mediated signaling (Ferrari, S. et al. 2007).

HGA degradation, with the release of OGs, is a mechanism evolved from the plants to monitor tissue injury. Pectin is the first component subjected to alteration or modification, thus explaining why specific and sophisticated mechanisms for sensing its integrity have been

evolved. These mechanisms are collectively indicated as ‘‘pectin integrity monitoring system’’ (PIMS) (De Lorenzo, G. et al. 2011). OGs have also been proposed as important signals in wound response (Bishop, P. D. and Ryan, C. A. 1987, Rojo, E. et al. 1999). Since they are negatively charged and have a limited mobility, their activity as a wound signal is likely to be restricted to the areas that are close to the damaged or wounded tissue (Baydoun, E. A. H. and Fry, S. C. 1985). Wound–inducible plant-derived PG genes, as described in tomato, may be responsible for a local production of endogenous OGs at the wounded site of the plant tissue (Bergey, D. R. and Ryan, C. A. 1999). OGs also regulate plant growth and developmental events in dicots (Altamura, M. M. et al. 1998, Bellincampi, D. et al. 1993, Bellincampi, D. et al. 1996, Branca, C. et al. 1988) and gymnosperms (Asiegbu, F. O. et al. 1994). Understanding how OGs are perceived is therefore necessary to elucidate their role *in vivo*, but the identification of an OG receptor has been daunting for a long time. With this regard, proteins belonging to the wall-associated kinases family (WAKs) were indicated as interesting candidates because of their ability to bind OGs and polygalacturonic acid (Anderson, C. M. et al. 2001, Decreux, A. and Messiaen, J. 2005). WAKs are receptor-like kinases, with an extracellular domain containing epidermal growth factor motifs, a transmembrane domain and an intracellular Ser/Thr

kinase domain (Anderson, C. M. et al. 2001). Arabidopsis has a small family of five WAK genes and a larger family of 22 WAK-like (WAKLs) genes (Verica, J. A. et al. 2003), though in monocots these families appear largely expanded (Zhang, S. et al. 2005). WAKs were first identified in Arabidopsis as pectin-bound proteins, since only harsh treatments, i.e., boiling in the presence of high concentrations of detergents and reducing agents or pectinase digestion could solubilize a protein reacting with an anti-WAK polyclonal antibody (He, Z. H. et al. 1996, Lally, D. et al. 2001, Wagner, T. A. and Kohorn, B. D. 2001). The ectodomains of WAK1 and WAK2 bind de-esterified HGA but not highly esterified HGA or other structurally different pectic components, such as rhamnogalacturonan I (RGI) and rhamnogalacturonan II (RGII; (Decreux, A. et al. 2006). Finally, through a chimeric receptor approach, it was established that WAK1 acts as a receptor of OGs (Brutus, A. et al. 2010).

PGIPs may also be considered players of the PIMS (De Lorenzo, G. and Ferrari, S. 2002, Sicilia, F. et al. 2005). PGIPs slow down the hydrolysis of homogalacturonan by microbial PGs and counteract the wall-breaching activity of these enzymes. Moreover, they favor the accumulation of elicitor active OGs, thus enhancing the plant alert system (De Lorenzo, G. et al. 2011). The importance of PGIPs in plant immunity has been established by several findings: transgenic

tomato and grape plants overexpressing a pear PGIP (Aguero, C. B. et al. 2005, Powell, A. L. T. et al. 2000) or transgenic tobacco and Arabidopsis plants overexpressing bean or Arabidopsis PGIPs exhibit enhanced resistance to *B. cinerea* infection (Ferrari, S. et al. 2003a, Manfredini, C. et al. 2005). Conversely, Arabidopsis plants expressing an antisense *pgip* gene showed increased susceptibility against *B. cinerea* (Ferrari, S. et al. 2006).

PGIP2 from *Phaseolus vulgaris* has been the first plant extracellular LRR protein to be characterized at the molecular, biochemical and structural level (Casasoli, M. et al. 2009, D'Ovidio, R. et al. 2004, De Lorenzo, G. 1994, Di Matteo, A. et al. 2006). It comprises 10 LRR motifs of the extracytoplasmic type (eLRR) characterized by the consensus sequence xxLxxLxLxxNxLt/sGxIPxxLGx. The eLRR motif is present in all the LRR RLKs, including FLS2 and EFR, and differs in terms of length and composition from those found in plant intracellular LRR proteins (Boller, T. and Felix, G. 2009).

1.2 Structural features of fungal polygalacturonases

Polygalacturonases produced by a large variety of bacteria, fungi and plants too, are involved in many physiological and pathological process, characterized by degradation and remodeling of the plant cell wall. Pathogenesis by fungi involves degradation of the

plant cell wall as a crucial event both to release compounds that are used as carbon sources by the fungus and to facilitate invasion, colonization and in many cases maceration of the host tissue. Fusarium spp. produce a great variety of cell wall degrading enzymes (CWDE) (Caprari, C. et al. 1996, de las Heras, A. et al. 2003, Jenczmionka, N. J. and Schafer, W. 2005, Ospina-Giraldo, M. D. et al. 2003). Endopolygalacturonases [poly (1,4-a-D-galacturonide) glycanohydrolase, EC 3.2.1.15; endoPGs] are among the first enzymes produced during infection (Garcia-Maceira, F. I. et al. 2001). Endo PGs degrade homogalacturonan to tri-, di-, and monogalacturonic acid as final products. Pectins are one of the main polysaccharides of middle lamella and primary cell walls in higher plants. However, partial degradation of the homogalacturonan leads to the release of oligogalacturonides (OGs), which are elicitors of plant defence responses (Hahn, M. G. et al. 1981). The interaction of endo PGs with plant cell wall polygalacturonase-inhibiting proteins (PGIPs) modulates their enzymatic activity and may favor the accumulation of elicitor-active OGs (Cervone, F. et al. 1989, De Lorenzo, G. and Ferrari, S. 2002). While fungi use PG as a component of their offensive arsenal to penetrate and colonize plant tissue (De Lorenzo, G. et al. 2001), plants, instead, utilize PGs in different process such as growth (Futamura, N. et al. 2000), fruit softening (Wang, Z. Y. et al. 2000), root formation, (Peretto, R. et al.

1992), pollen development (Allen, R. L. and Lonsdale, D. M. 1993) and organ abscission (Kalaitzis, P. et al. 1997). The complex role of PGs in the plant cell wall remodeling, is documented by the presence of large PG gene families in plant genomes: more than 50 putative PGs gene, have been identified in *Arabidopsis thaliana* (Torki, M. et al. 1999). Fungal PGs with an *endo* mode of action, hydrolyze 1-4 linkages between two α-D-galacturonic acid residues. The mode of action of endo-PGs may be either by a single chain multiple attack mechanism, in which end products appear rapidly, or by a multi-chain attack, where the monomers, dimer and trimers accumulate only after further hydrolyses of oligogalacutornides. For example the PG secreted by *Colletotrichum lindemuthianum* produces only di- or trigalaturonic acids (English, P. D. et al. 1972), while the PG from *Saccharomyces fragilis* hydrolyzes pectin until mono and digalacturonic acids (McClendon, J. H. 1979). The endo PG produced by *Fusarium phyllophilum*, the best characterized endo-PG, hydrolyses the linkages between two galacturonic acid residues by a multi-chain attack mechanism (Bonnin, E. et al. 2002). This PG cleaves the trigalacturonic acid (GalA3), but not the dimer and the reaction velocity increased with chain length. GalA3 was cleaved according to a 2+1 mode. This indicates the location of the catalytic site with respect to the three subsites binding GalA3, which could be referred to as -2/+1 according to the nomenclature proposed by

Davies et al. (1997). As it was demonstrated that the digalacturonic acid (GalA2) was not a substrate, it can be deduced that subsite -2 plays a critical role in the formation of a productive complex. Fungal endo PGs also show considerable differences in action patterns on oligogalacturonides. These differences depend on the nature of the active site, but more specifically on the size of the substrate and the position of the catalytic group (Rexova-Benkova, L. 1973). *Aspergillus niger* produce 7 PGs, three of them, PG I, II and C are well characterized: these PGs cleave the polygalacturonate in an endo type mode of action (Benen, J. A. E. et al. 1999). All three enzymes cleaved these oligogalacturonides from the reducing end with different rates, and the minimum number of subsites is seven for all three enzymes. Comparison of the available polygalacturonase sequences from bacterial, fungal, and plant origin reveals that only eight amino acid residues are strictly conserved (Kester, H. C. M. et al. 1996). These residues are: Asn^{178}, Asp^{180}, Asp^{201}, Asp^{202}, His^{223}, Gly^{224}, Arg^{256}, and Lys^{258} (sequence numbering according to *A. niger* PGII). The eight conserved residues form a predominantly negatively charged patch in the cleft. Asp^{201} is proposed to act as the acid (proton donor), while Asp^{180} and Asp^{202} activate the hydrolytic water molecule on the digalacturonic acid molecule (fig.4) (Bonnin, E. et al. 2002, van Santen, Y. et al. 1999).

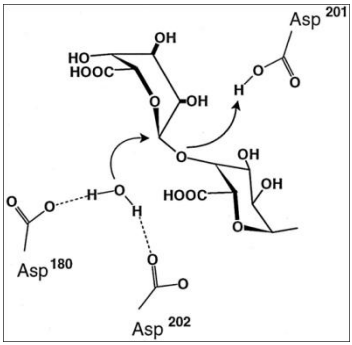

Figure 4. Schematic representation of the catalytic mechanism proposed for the endo polycalaturonase II of *A. niger*.

The conserved Asp^{201} (*A. niger* endo polygalacturonase numbering) acts as the proton donor, while Asp^{180} and Asp^{202} activate the hydrolytic water molecule. (Adapted fron van Santen *et al.*, 1999).

van Santen et al. (1999) solved the crystal structure of PG II from *A. niger*: (AnPGII), this enzyme is folded into a right-handed parallel β-helical structure comprising 10 complete turns (fig.5 A). The number of amino acids per turn varies from 22 to 39, averaging to 29 residues per turn. This variation is caused by the diversity of lengths of the loops connecting theβ-strands. The β-helix is formed by four parallel β-sheets, named PB1, PB2a, PB2b, and PB3. This naming was adopted to be consistent with the naming of the β-sheets in the pectate lyase structure, the first right-handed parallel β-helical structure that was solved (Yoder, M. D. et al. 1993). The turns between the β-helical strands are named based on the sheets they connect. The turns between PB1 and PB2 (a or b) are referred to as

T1-turns, between PB2 (a or b) and PB3 as T2-turns, and between PB3 and PB1 as T3-turns. The T1-turns are relatively longer near the C-terminal side of the β-helix, whereas the T3-turns are longest near the N-terminal side of the b-helix. In this way the loops form two bulky extensions on the exterior of the β-helix (fig. 5 B).

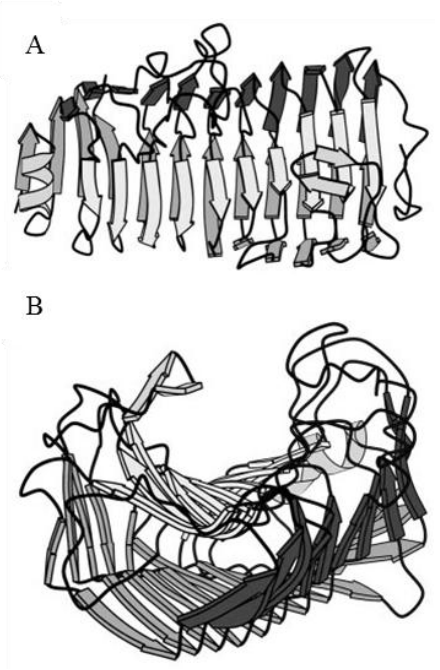

Figure 5. Three-dimensional structure of endopolygalacturonase II from *Aspergillus niger*

A) The N terminus on the left and the C terminus on the right, viewed onto β-sheet PB1 (light gray). PB2a and PB2b are shown in gray, and PB3 is shown in dark gray. B) The structure viewed from the C-terminal side, showing the cleft that is formed by the loop regions T1 (left side loop region) and T3 (right side loop region). (Adapted from van Santen *et al.*, 1999).

Between these extensions a large cleft is present: the cleft is approximately 8 Å wide, and well suited to accommodate the unbranched polygalacturonan substrate. The essential catalytic residues, Asn^{178}, Asp^{180}, Asp^{201}, Asp^{202}, His^{223}, Gly^{224}, Arg^{256}, and Lys^{258}, are located in this cleft. Federici et al. (1999) have solved the crystal structure of another endo-PG: the PG produced by phytopathogenic fungus *Fusarium phyllophilum* (FpPG; fig.6). The overall architecture consists of a right-handed parallel β-helix, resulting from the tandem repetition of 10 coils, each formed by three or four β-strands The β-strands of consecutive turns line up to form parallel β-sheets indicated as PB1, PB2a, PB2b, and. The β-sheet PB2a, starting from the sixth turn of the α-helix, is typical of PGs and is absent in other proteins sharing the same overall fold (Pickersgill, R. et al. 1998).

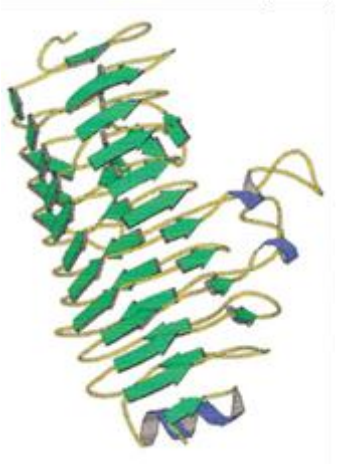

Figure 6. Structure of FpPG.
Schematic representation of the right handed parallel β-helix, consisting of 10 coils each made up of three or four β-strands (green). (Adapted from Federici *et al*., 2001)

The length of the β -strands is generally short (3 to 5 residues); more variable is the length of the turns (T) between β-strands. The turns T1 (between PB1 and PB2b or PB2a) and T2 (between PB2b and PB3), and the PG-specific turns between PB2a and PB2b, are very short. The T3 turns (between PB3 and PB1) are more variable, and their length varies from 3 to 24 residues; these loops, as for the AnPGII, determine the formation of a deep cleft on one side of the β-helix, where the putative active site is located. FpPG and AnPGII have a sequence identity of 43.5%, and their structures are almost completely superimposable. All secondary structure elements are conserved among the two proteins both in the β-helical region and in

the region outside the β-helix (fig. 7). Thirteen of the 15 additional residues of FpPG form two loops that are absent in AnPGII.

Figure 7. Superimposition between FpPG and AnPGII.
Structural superposition between FpPG (in red) and AnPGII (in blue) represented as protein ribbons. (Adapted from Federici *et al*., 2001)

1.3 Polygalacturonase inhibiting protein (PGIP)

Many plants produce extracellular PGIPs that specifically recognize and inhibit fungal PGs (De Lorenzo, G. and Ferrari, S. 2002, Mariotti, L. et al. 2009). The PG-PGIP interaction limits the

destructive potential of polygalacturonase and leads to the accumulation of active oligogalacturonides (Ridley, B. L. et al. 2001).

The overexpression in Arabidopsis of the genes A*tpgip1* and *Atpgip2* limits the colonization by *B. cinerea* and reduce symptoms disease (Ferrari, S. et al. 2003b). A significant increase of PG-inhibitory activity and a decrease in susceptibility to *B. cinerea* has been found in transgenic tomato and grapevine plants overexpressing a pear pgip (Aguero, C. B. et al. 2005, Powell, A. L. T. et al. 2000), and in tobacco or Arabidopsis plant overexpressing PGIP2 from *Phaseolus vulgaris* (PvPGIP2) (Manfredini, C. et al. 2005). To accommodate pathogenesis for different environmental conditions and on various hosts, fungi produce PG isoenzymes variable in terms of sequence, specific activity, pH optimum and substrate preference (De Lorenzo, G. et al. 2001, Poinssot, B. et al. 2003). Conversely plant have evolved PGIPs with different recognition specificities encoded by differentially regulated pgip gens (De Lorenzo, G. and Ferrari, S. 2002, Ferrari, S. et al. 2003b).

The crystal structure of PvPGIP2 was determined (Di Matteo, A. et al. 2003); PvPGIP2 shows the right-handed superhelical fold typical of LRR proteins such as the porcine and humane ribonuclease inhibitors (Kobe, B. and Deisenhofer, J. 1993), internalin B (Marino, M. et al. 1999) and decorin (Scott, P. G. et al. 2004). The fold of

PvPGIP2 consists of a central LRR domain, flanked by the N- and C-terminal cysteine rich regions (fig. 8).

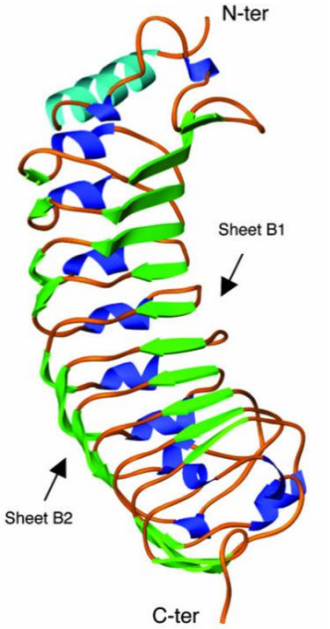

Figure 8. Structure of PGIP2 from *P. vulgaris.*

Ribbon representation of the structure of PGIP2. Sheets B1 and B2 are colored green, and helices are colored blue (light blue for the N-terminal α-helix and dark blue for 3_{10}-helices in the LRR central portion of the molecule) (Adapted from Di Matteo, A. et al., 2003).

The LRR domain is characterized by the tandem repetition of 10 coils matching the consensus sequence xxLxLxxNxLt/sGxIPxxLxxLxxL. An extended parallel β-sheet (B1), conserved in all known LRR protein structures (Kobe, B. and

Kajava, A. V. 2001), occupies the concave inner side of the protein solenoid. B1 is the β-sheet where the residues determining the affinity and specificity of PGIP3 reside (Leckie, F. et al. 1999, Sicilia, F. et al. 2005). PvPGIP2 has an additional parallel β-sheet (B2) that is distorted because of the twisted shape of the molecule and the variable length of the β-strands. Specific position of the LRR repeats, are occupied by hydrophobic amino acids, mostly leucine, that point into the interior of the protein scaffold and stabilize the overall fold topology through van der Waals interactions. The convex face of the LRR region of PGIP2 is mostly occupied by unstructured segments that are stabilized through water molecules; these are organized in spines along the structure and form H-bond interaction with the protein backbone (Evdokimov, A. G. et al. 2001, Marino, M. et al. 2000).

1.4 The PG-PGIP interaction

PGIPs specifically interact with PGs by forming a bimolecular complex (De Lorenzo, G. et al. 2001). The PG-PGIP interaction varies in term of inhibition kinetics and strength, and reflects the counter-adaptation occurring in both enzymes and inhibitors. Pathogens have evolved different PGs to maximize their offensive potential and, conversely, plants have evolved various

PGIPs with different specificities to counteract pathogen PG structural adaptation. For instance PGs from *B. cinerea* (BcPGs) and *Collethotricum acutatum* are inhibited with different efficiencies by all members of the bean PGIP family, while PG from *A. niger* is inhibited by PvPGIP1 and PvPGIP2 but not by PvPGIP3 or PvPGIP4 (D'Ovidio, R. et al. 2004). PG from *Fusarium phyllophilum*, is inhibited only by PvPGIP2 (Leckie, F. et al. 1999). PGs from the phytophagous insect *Lygus rugulipennis* and *Adelphocoris lineolatus* are inhibited only by PvPGIP3 and PvPGIP4 (D'Ovidio, R. et al. 2004). Variability of recognition and function of PGIPs is not only reflected by their specificity but also by the variable inhibition kinetics played against different fungal PGs: tomato PGIP inhibits AnPGII in a non-competitive manner (Stotz, H. U. et al. 2000); PGIPs from bean (Lafitte, C. et al. 1984) and raspberry (Johnston, D. J. et al. 1993) are non-competitive inhibitors of PG from *Collethotricum lindemuthianum* and *B. cinerea* respectively. PvPGIP2 acts competitively against FpPG (Federici, L. et al. 2001), non-competitively against AnPGII (King, D. et al. 2002) and by a mixed mode of inhibition against BcPG1 (Sicilia, F. et al. 2005). Computational analysis predicts that the hyper variable LxxLxLxx region spanning the sheet B1 in the concave surface of PvPGIP2 has a strong propensity to be engaged in protein-protein interactions (Federici, L. et al. 2006, Sicilia, F. et al. 2005); this is the same area

where the determinants of PGIPs affinity and specificity are located (Casasoli, M. et al. 2009, Leckie, F. et al. 1999, Sicilia, F. et al. 2005). Homologous regions of other LRR proteins such as the ribonuclease inhibitor (Stumpp, M. T. et al. 2003) and internalin A (Schubert, W. D. et al. 2002) are also involved in recognition. Sheet B1 is the surface of PvPGIP2 containing several residues critical for affinity and recognition capability: in particular the negative pocket formed by three aspartic acid residues (Asp^{131}, Asp^{157} and Asp^{203}) located approximately in the middle of sheet B1 is important for inhibition of the *F. phyllophilum* PG and probably interacts with the positively charged cleft of the enzyme (Spinelli, F. et al. 2009). Benedetti et al. (2011) have analyzed the interaction between FpPG and the PvPGIP2 using small-angle X-ray scattering (SAXS) combined to site-directed mutagenesis and inhibition assays. SAXS is a method for the analysis of biological macromolecules in solution that, due to the progress in computational methods of the last decade, has become a powerful tool to decipher three-dimensional low-resolution structures (Koch, M. H. et al. 2003, Lipfert, J. and Doniach, S. 2007, Svergun, D. I. et al. 2001). PvPGIP2 interacts with the enzyme by means of the concave surface of its LRR scaffold. An extended surface of PvPGIP2 accounting for 810 Å is buried during the formation of the complex with FpPG (fig.9).

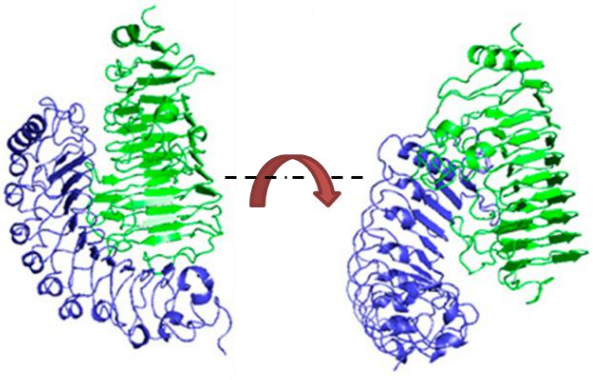

Figure 9. FpPG-PvPGIP2 SAXS model.
Three-dimensional structure of the chemically cross-linked complex between FpPG (in green) and PvPGIP2 (in blue). Two orthogonal viewpoints are reported (Adapeted from Benedetti, M. et al., 2011).

This area comprises residues belonging to the 10 LRRs of the inhibitor and therefore spans over the entire LRR domain. The enzyme and inhibitor interact in a head to-head orientation with the two N termini located on the same side. It is worth noting that some of the inhibitor residues appearing as contact points in the SAXS structure, have been previously predicted to be subjected to positive selection by codon variation analysis and to possess favorable desolvation energy for protein-protein interactions (Casasoli, M. et al. 2009).

1.5 WAKs family

The wall-associated kinases (WAKs) are RLKs that are tightly bound to the cell wall (He, Z. H. et al. 1996). There are five highly conserved *WAK* genes in Arabidopsis, all clustered in chromosome 1 and additional 26 *WAK*-like genes that encode proteins with divergent extracellular domains than the WAK family (Verica, J. A. et al. 2003). The five WAKs are expressed in a variety of tissues with WAK1 and WAK2 being the most abundant (He, Z. H. et al. 1996, Wagner, T. A. and Kohorn, B. D. 2001). *WAKs* are expressed in germinating seedlings and at most tissue junctions; expression is detected in all layers of the apical meristem and leaf primordial and it is induced within minutes from wounding and within hours after aluminum toxicity, pathogen and numerous other stresses (He, Z. H. et al. 1998, Sivaguru, M. et al. 2003, Wagner, T. A. and Kohorn, B. D. 2001). WAKs have been implicated in the plant's response to pathogens, as their NPR1-dependent expression is required during the pathogen response, and expression of the WAK kinase domain can lead to salicylate resistance (He, Z. H. et al. 1998).

The five WAKs proteins consist of an extracellular domain, a transmembrane domain and an intracellular Ser/Thr protein kinase domain (Shiu, S. H. and Bleecker, A. B. 2003) (fig 10). The extracellular domain of WAKs are only 40–64% identical. This

identity is in clusters and all WAKs contain conserved EGF-like cysteine repeats (He, Z. H. et al. 1999) (He, Z. H. et al. 1996).

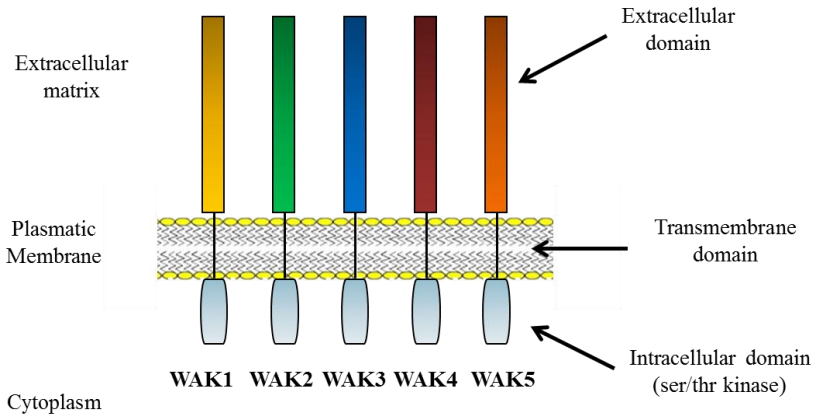

Figure 10. Simplified representation of the five wall-associated kinases. The WAK isoforms share the same structure and are 87% identical in their cytoplasmic kinase (blue). Their amino termini are linked to the cell wall and all contain EGF repeats (lightest green) adjacent to the transmembrane domain (red). The extracellular regions are 40–64% identical among isoforms and the differences are depicted by the various colors (Adapeted from Anderson *et al*., 2001).

The function of these repeats is unknown and, surprisingly, they constitute one of only a few examples (Laval, V. et al. 1999) found in the plant kingdom. In metazoans, EGF repeats aid in the calcium-mediated dimerization of proteins, often receptors (Zhang, Y. et al. 1998). WAK1 and WAK2 contain, in the non EGF portion of the extracellular region, a so-called Pectin Binding Domain (PBD) for which no structural homologues are available (Decreux, A. and Messiaen, J. 2005). The serine/threonine kinase domains of the five

WAK proteins share 86% amino acid identity and they all contain the eleven conserved regions of serine/threonine kinases (He, Z. H. et al. 1998, Wagner, T. A. and Kohorn, B. D. 2001). WAKs are required for cell expansion during plant development. Disruption of WAK function using inducible expression of full-length WAK2 antisense RNA, which likely disrupts multiple WAKs, compromised leaf cell expansion (Lally, D. et al. 2001, Wagner, T. A. and Kohorn, B. D. 2001). Consistent with these results, root cell elongation is impaired in wak2 loss-of-function mutants and in seedlings expressing WAK4 antisense RNA (Kohorn, B. D. et al. 2006b, Lally, D. et al. 2001). The growth of a wak2 loss-of-function mutant was dependent on exogenous sugars, suggesting that the mutation may alter sugar metabolism (Kohorn, B. D. et al. 2006b). This idea is supported by the finding that wak2 mutant roots show reduced vacuolar invertase activity, which is critical for the generation of solutes required to maintain turgor pressure during cell expansion (Kohorn, B. D. et al. 2006b). WAKs were not significantly expressed in the elongation zone of roots, the inflorescence stem, cauline leaves and flower organs other than the base, sepals and ovaries (He, Z. H. et al. 1996, Wagner, T. A. and Kohorn, B. D. 2001). *Wak1*, *Wak2*, *Wak3* and *Wak5* are mainly expressed in green organs (leaves and stems). A trace amount of Wak1 and Wak2 transcripts can also be found in flowers and siliques. A low amount of Wak2 transcript is

detectable in roots and Wak4 mRNA is found only in siliques (He, Z. H. et al. 1998).

1.6 WAK1 is bound to pectin

The interaction of WAK1 with cell wall pectins was first reported by He et al. (1996). The use of harsh extraction conditions (4 % SDS, 50 mM DTT and boiling) or heavy pectinase treatments (Wagner, T. A. and Kohorn, B. D. 2001) to release WAK1 from the cell walls, led to the conclusion that WAK1 was covalently bound to pectin. (Decreux, A. and Messiaen, J. 2005).

He et al. (1996) proposed that WAK1 could be ionically bound to calcium-associated homogalacturonans, forming a tuneable complex during cell wall turn-over or plant-microbe interactions.

A specific region of the extracellular domain of WAK1, corresponding to amino acids 67–254 binds calcium-induced homogalacturonan dimers and multimers (Decreux, A. et al. 2006). Using truncated versions of the full-length extracellular domain of WAK1, Decreux and Messiaen, (2006) found that most of the homogalacturonan- binding activity of WAK1 is located near the N-terminal end of the extracellular domain of WAK1, between amino acid residues 2–111 (70% of the binding activity of WAK67–254). Within this domain, five basic amino acids (R67, R91, K101, K102

and R166) are involved in the interaction with negatively charged homogalacturonans (Anderson et al., 2001).

1.7 WAK1 localization

He et al. (1996) tried to localize in the plant cell WAK1 by immunocytochemistry; localization by light microscopy revealed that WAK1 is bound to the surface of all cells. The dynamics of WAK1 localization was studied by Kohorn et al. (2006a) following a fluorescent WAK1 fusion protein (WAK1-GFP), expressed in mesophyll protoplasts isolated from Arabidopsis. Expression of WAK1-GFP, leads to the accumulation of the fusion protein in a cytoplasmic compartment that also contains pectin, and the detection of this compartment depends upon WAK1-GFP expression. Furthermore, co-localization studies between WAK1-GFP and Jim 5, an anti-pectin serum that recognizes homogalacturonan, (Willats, W. G. et al. 2000), showed that WAK1 is on the surface of compartments that contain pectin, and these compartments have a varied surface contour (fig. 11). WAK1-GFP, also, colocalizes with markers for the Golgi, indeed the site of pectin synthesis, but does not colocalize with markers of the endosome or vacuoles.

1.8 WAK1 as the OGs receptor

Brutus et al. (2010) recently demonstrated that WAK1 is a OG receptor, by using chimeric proteins. Two different EFR based-chimeras, to dissect the functionality of WAK1, named WEG (WAK-EFR) and EWAK (EFR-WAK) were designed and transiently expressed in tobacco leaves and stably in the Arabidopsis *efr* mutant. Responses differentially induced by OGs and elf18 were analyzed, including ethylene accumulation, which is induced by elf18 but not by OGs, and expression of gene markers up-regulated by elf18 (and flg22) but not by OGs (Zipfel, C. et al. 2006). Both WEG and EWAK were activated specifically by OGs and elf18, respectively, to trigger PTI, in both plant species (Brutus, A. et al. 2010). Transgenic plants overexpressing WAK1 clearly indicated that this receptor has a function in defense. These plants, which show levels of WAK1 transcripts about ten times higher than those present in untransformed plants, exhibit enhanced responsiveness to OGs and increased resistance to *B. cinerea* (Brutus, A. et al. 2010).

2. AIM OF THE THESIS

Pectin is the outer component of the plant cell wall and, therefore, is among the first structures to be challenged during pathogen invasion or wounding (De Lorenzo, G. and Ferrari, S. 2002). To gain access to the plant tissue, pathogens secrete cell wall-degrading enzymes (CDWEs), including endo-polygalacturonases (PGs) that cleave the α-1,4 linkages between D-galacturonic acid residues in the homogalacturonan causing cell separation and maceration of the host tissue (Cantu, D. et al. 2008). Nowadays the PGs are considered as virulence factor (Rodriguez-Palanzuela et al., 1991).

The first aim of this thesis was to analyze the PG secreted from *Fusarium verticillioides* (FvPG) by structural and biochemical approaches. *Fusarium* species are the asexual state of *Giberella* species (Desjardins et al., 1989). Most *Fusarium* are destructive plant pathogens; they cause head blights of *Triticum aestivum* (wheat), ear rots of *Zea mays* (maize), bakanae disease of *Oryzae sativa* (rice), tuber dry rot of *Solanum tuberosum* (potato), and pitch canker of Pinus species (Desjardins, A. E. et al. 1996, Desjardins, A. E. et al. 2006). *F. verticillioides* is associated with disease at all stages of corn plant development infecting the roots, stalk and kernels and symptomless infection can exist throughout the plant in leaves, stems, roots, grains and the presence of the fungus is in many cases

ignored because it does not cause visible damage to the plant (Battilani, P. et al., 2003); *F. verticillioides* is likely to be the most common species isolated worldwide from diseased maize (Desjardins, A. E. and Hohn, T. M. 1997).

We have stated previously that the PG-PGIP interaction is paradigmatic for studying the key recognition events that underlie plant immunity (Misas-Villamil, J. C. and Van der Hoorn, R. A. 2008). Importantly, *Fusarium verticilloides* secretes only one PG (FvPG) that is 92.5% identical to the PG secreted from another fungus of the same genus, *Fusarium phyllophylum*, with only 30 amino acid variations over 373 residues in the mature enzymes. Despite this high conservation, PGIP2 from *Phaseolus vulgaris* (PvPGIP2) is unable to inhibit FvPG (Mariotti, L. et al. 2009, Raiola, A. et al. 2008), while it is able to inhibit, very well, the FpPG. Likewise FvPG is not inhibited by any PGIP characterized so far.

Here I resorted to better inderstand the structural basis for the lack of inhibition by PvPGIP2 on FvPG activity. To this aim, a better characterization of the amino acids involved in the PG-PGIP complex formation is necessary as well as knowledge of the 3D structure of FvPG. Recently, a low resolution structure of the complex formed by PvPGIP2 and FpPG was determined by Small-Angle X-ray Scattering (SAXS) (Benedetti, M. et al. 2011); this allowed to pinpoint the residues involved in the FpPG-PvPGIP2

interaction. Determination the 3D structure of the FvPG could be useful to compare it with the, already known, 3D structure of FpPG; and the combination of these structural data with those obtained by SAXS, would suggest which amino acids of the FvPG are responsible for the lack of inhibition by PvPGIP2. To determine the 3D structure of the PG from *F. verticillioides*, I used a X-Ray crystallography approach, after expression of the protein in the heterologous system *Pichia pastoris*, to obtain a high amount of protein.

In the second part of my thesis I've performed a structural and biochemical study on the Wall Associated Kinese 1 (WAK1) protein. The perception of OGs, released upon wouding or degradation by CWDEs (like PGs) suggests that they act as indicators of the integrity of the tissue during normal and adverse conditions. Constant and dynamic interactions between cells and their cell walls are emerging as important regulatory mechanisms for plant growth, development and immunity. With their ability to interact with cell walls, pectin and OGs, WAKs appear as key elements in the communication of cells with the external microenvironment (De Lorenzo, G. et al. 2011). Recently it has been demonstrated, by Brutus et al., (2010) that a member of the WAK family, WAK1, is a receptor for the OGs. Plants overexpressing WAK1 are more resistant to *B. cinerea* and *Erwinia carotov0ra*, two important

pathogens of plants (Brutus, A. et al., 2010). Until now, no studies have been performed to describe, at a structural level, the link between OGs and WAK1. Solving the three-dimensional structure of this receptor, could pave the way to charachterize the binding of WAK1 to OGs. For this reason the main aim of this part of the thesis was to express the protein in high yields for subsequent structural analysis.

While the cytosolic kinase domain of WAK1 is highly homologous to those of several proteins already determined and available in the Protein Data Bank, the situation is different for the ectodomain. This domain can be divided in to a N-terminal pectin binding domain (PBD) and two EGF-like domains. Structures for domains homologous to the WAK1 EGF-like domain are available in the Protein Data Bank. Conversely, nothing is known about the structure of the PBD.

Here, I verified the possibility to express and purify the isolated ectodomain of WAK1 (eWAK1) that include the PBD and the two EGF-Like domains, from two heterologous systems, *Pichia pastoris* and *Nicotiana tabacum*, for subsequent structural studies. A characterization of the folding properties of the the protein expressed in both ways, was also performed.

3.RESULTS

3.1 Expression in the heterologous system *Pichia pastoris* and purification set-up of FvPG

The endo-polygalacturonase produced by *F. verticillioides* (FvPG) shares an high amino acid identity (93%) with the PG secreted by *Fusarium phyllophylum*, whose 3D structure has already been solved (Federici, L. et al. 2001). The FpPG is inhibited by PGIP2 of *Phaseolus vulgaris* (PvPGIP2), while the FvPG is not inhibited neither by PGIP2 nor from other PGIP characterized so far (Mariotti, L. et al. 2009)

For crystallographic studies it is necessary to have a high amount of purified protein; for this purpose the expression of the FvPG was performed in the heterologous system *Pichia pastoris*. The entire *FvPG* gene, (fig. 11) was amplified by PCR, using the primer FvPGEcoFw and FvPGXbaRev (See table II in Materials and methods) to introduce in the gene the two resctrtion sites *EcoRI* and *XbaI* in the 5'- and 3'-terminal ends of the gene, respectively. The PCR product and the vector used for cloning, pGAPZα, was digested with the two restriction enzymes, purified, ligated and transformed by electroporation in *E. coli*. Then the recombinant vector, pGAPZα.FvPG, extracted from *E. coli*, was linearized by the restriction enzyme AvrII, needed for the site-specific recombination

in *P. pastoris*. The FvPG gene is fused upstream with the sequence encoding the α-factor signal peptide contained in the vector pGAPZα that allows constitutive expression in *P. pastoris* (fig. 36).

```
1          GATTCGATCCCTGCTCCGTGACTGAGTACTCCGGCCTCGCCACCGCCGTCTCATCCTGCA
1             F  D  P  C  S  V  T  E  Y  S  G  L  A  T  A  V  S  S  C

61         CAAACATCGTTCTCGCCGGCTTTCAAGTCCCGACAGGCAAGCAACTTGATCTATCCAAGC
20         T  N  I  V  L  A  G  F  Q  V  P  T  G  K  Q  L  D  L  S  K

121        TCAAGGCTGGCACAACCGTCACTTTCAAGGGCAAGACCACTTTTGCCACCACTGCTGACA
40         L  K  A  G  T  T  V  T  F  K  G  K  T  T  F  A  T  T  A  D

181        ACGACTTTGATCCTATCGTCATCAGTGGGAGTGGTATCACCATAACTGGTGCATCTGGTC
60         N  D  F  D  P  I  V  I  S  G  S  G  I  T  I  T  G  A  S  G

241        ATGTCATTGACGGCAACGGTCAAGCGTACTGGGACGGCGAAGGTTCCAACAACAAGGACA
80         H  V  I  D  G  N  G  Q  A  Y  W  D  G  E  G  S  N  N  K  D

301        ACCCCAAGCCTGACCACTTCATCGTTGTCAAGAAGACCACCGGCAACTCAAAGATCACAA
100        N  P  K  P  D  H  F  I  V  V  K  K  T  T  G  N  S  K  I  T

361        ACCTCAACATCCAGAACTGGCCCGTTCACTGCTTCGACATCACCGGCAGTTCACAATTAA
120        N  L  N  I  Q  N  W  P  V  H  C  F  D  I  T  G  S  S  Q  L

421        CCATCTCAGGGCTAATTCTTGACAACAGAGCCGGTGACAAGCCAAATGCCAAGAGCGGTA
140        T  I  S  G  L  I  L  D  N  R  A  G  D  K  P  N  A  K  S  G

481        GCTTGCCCGCTGCGCATAACAGCGACGGTTTCGACATTTCGTCCAGCGACCACGTCACTC
160        S  L  P  A  A  H  N  S  D  G  F  D  I  S  S  S  D  H  V  T

541        TGGATAATAACCATGTTTATAACCAGGATGATTGCGTTGCCGTCACTTCTGGTACCAACA
180        L  D  N  N  H  V  Y  N  Q  D  D  C  V  A  V  T  S  G  T  N

601        TCGTTGTTTCAAACATGTATTGCTCCGGCGGTCATGGCCTTAGTATCGGATCTGTTGGTG
200        I  V  V  S  N  M  Y  C  S  G  G  H  G  L  S  I  G  S  V  G

661        GAAAGAGCGACAATGTCGTCGATGGTGTTCAGTTCTTGAACTCGCAGATTGTGAACAGTG
220        G  K  S  D  N  V  V  D  G  V  Q  F  L  N  S  Q  I  V  N  S

721        AGAATGGATGTCGCATCAAGTCCAACTCTGGAACAACTGGCACGATCAACAACGTTACCT
240        E  N  G  C  R  I  K  S  N  S  G  T  T  G  T  I  N  N  V  T

781        ACCAGAACATTGCTCTTACCAACATCAGCAAATACGGTGTCGATGTCCAGCAAGATTATC
260        Y  Q  N  I  A  L  T  N  I  S  K  Y  G  V  D  V  Q  Q  D  Y

841        TCAACGGCGGTCCTACTGGAAAGCCCACCAACGGAGTCAAGATCAGCAATATCAAGTTCA
280        L  N  G  G  P  T  G  K  P  T  N  G  V  K  I  S  N  I  K  F

901        CCAAGGTTACTGGAACCGTGGCCAGCTCAGCTCAGAACTGGTATATTCTGTGCGGTGATG
300        T  K  V  T  G  T  V  A  S  S  A  Q  N  W  Y  I  L  C  G  D

961        GTAGCTGCTCTGGATTTACCTTTTCAGGAAACGCTATCACCGGCGGCGGCAAGACTAGCA
320        G  S  C  S  G  F  T  F  S  G  N  A  I  T  G  G  G  K  T  S

1021       GCTGCAACTATCCTAGCAACACTTGCCCCAGCTAG
340        S  C  N  Y  P  S  N  T  C  P  S  *
```

Figure 11. The entire nucleotidic and amino acidic sequence of the FvPG.

In the upper line is reported the entire nuclotidic sequence of the *FvPG* gene, while in the lower line, the amino acid sequence.

The FvPG protein has a theorethical molecular weight of about 36 kDa, and an isoelectric point (pI) of 5.94, both calculated with a program available on line (http://web.expasy.org/cgi-bin/protparam/protparam). Along the amino acid sequence, shown in figure 10, it is possible to find two putative N-glycosilation sites, predicted by the online server NetNGlyc (http://www.cbs.dtu.dk/services/NetNGlyc/).

The *P. pastoris* transformants, were analyzed by PCR, using the primers FvPGEcoFw and FvPGXbaRev. Three *P. pastoris* colonies, positive for PCR, were inoculated into YPD medium (see Materials and Methods for the composition of the medium) and grown for 24 hours at 28° C. The culture filtrates from positive colonies were analyzed by western blotting, using an anti-FpPG antibody: in the western bloting showed in figure 12 A, appear a double band, in each line of the trasformants (1 to 3), with a molecular weight of about 36 kDa, confirming that the protein was expressed. The double bands represent two different glycoforms of the FvPG protein, as already known for other PGs expressed in Pichia (see positive control in fig. 12 A). As positive control of the western blotting, a culture filtrate of *P. pastoris* expressing the FpPG was used; this protein also is expressed in two glycoforms.

To test if the expressed FvPG is functional, the enzymatic activity of the culture filtrate was analyzed by agar diffusion assay. The halo

around each well, shows the polygalacturonase activity of FvPG, after 24 h of incubation in the agar with polygalacturonic acid, and revealed with 6 M HCl (fig. 12B).

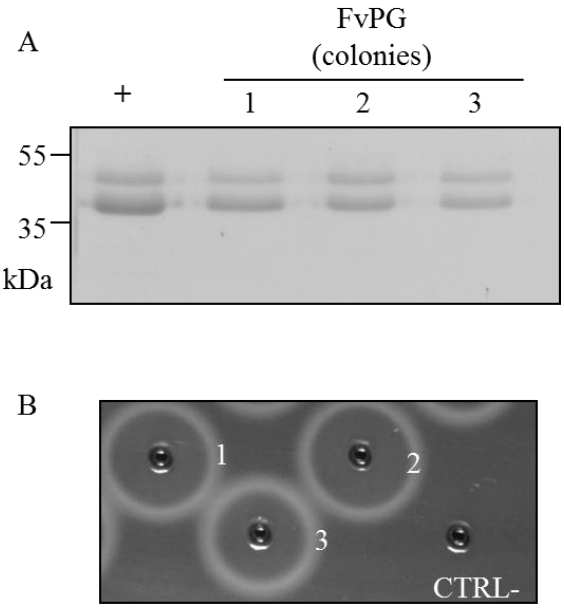

Figure 12. Analysis of the expression of FvPG in *P. pastoris.*
A) Three *Pichia* trasformants were analyzed by Western blotting: 20 µL of culture filtrate were analyzed using an anti-FpPG polyclonal antibody; each trasformant express the FvPG (line 1 to 3). Culture filtrate of *P. pastoris* expressing FpPG, was used as a positive control. B) Polygalacturonase activity, was detected by agar diffusion assay, in the culture filtrate of the three *Pichia* trasformants (well 1 to 3); no activity was detected in the non trasformed *Pichia* cell (CTRL-).

The *Pichia* transformed colony expressing a greater extent of FvPG, as shown by Western blotting, was choosen for the massive production of the protein: the colony number 3, was inoculated in 2

liters of YPD and grown for three days at 28° C. The culture filtrate was separated from the *Pichia* cells by centrifugation and concentrated using a Tangential Crossflow Concentrators (Vivaflow 200 Sartorius); the concentrate obtained, was purified through three different chromatographic techniques, as described for the FpPG by Federici et al., (2001), according to the theoretical molecular weight and pI. The purification step can be summarized in the flow-chart showed in figure 13.

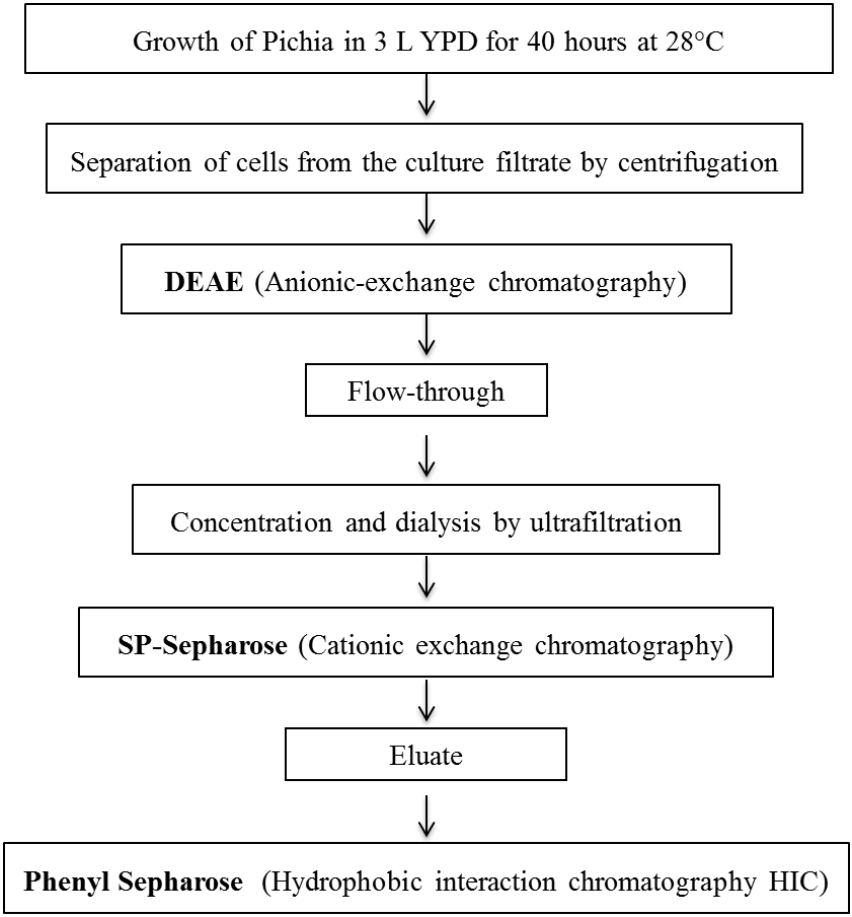

Figure 13. Flow-chart of the FvPG purification

After each chromatographic step, the fractions eluted from the columns, was separated by SDS-PAGE and stained with coomassie

blue to assess the presence of the protein and the degree of purification (fig 14).

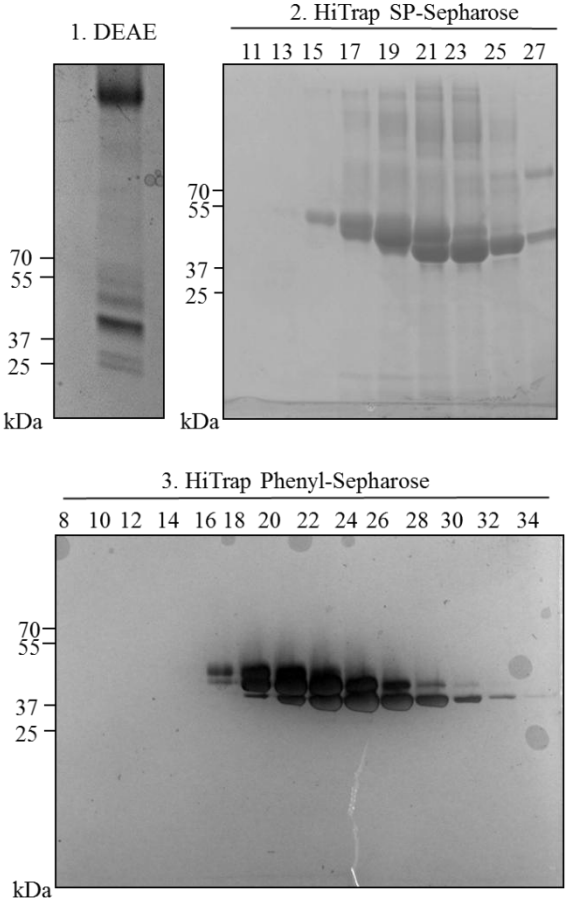

Figure 14. SDS-PAGE analysis oon the purfied FvPG from *P. pastoris*
The eluted fractions were separated with SDS PAGE and stained with coomassie blue. The number indicates the different fraction eluted from each columns.

After each step of purification, the purity of the protein increases, and in the eluate of the last column, FvPG was the only protein observed, in its two glycoforms, with a purity degree higher than 90%. The purified fractions containing FvPG eluited from the HiTrap Phenyl Sepharose column, were pooled and concentrated to obtain a final concentration of 12 mg L^{-1}. To further confirm that the purified protein is FvPG, and that this is functional, I have analyzed the protein by western blotting, using an anti-FpPG antibody, and by agar diffusion assay to evaluate the activity of the protein, in the absence or presence of PvPGIP2 (fig.15 A and B)

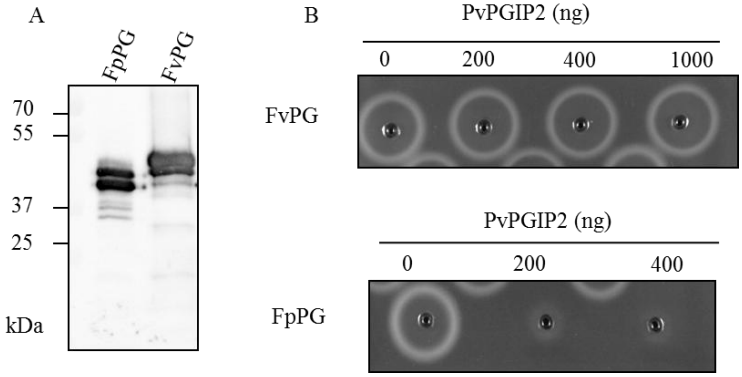

Figure 15. Analysis of the purfied FvPG from *P. pastoris.*
A) Western blotting analysis of purified FvPG, using an anti-PG polyclonal antibody. FpPG expressed and purified by P. pastoris, was used as a positive control. B) Inhibitory activities of PvPGIP2 against the purified FvPG (3 ng) or FpPG (1,5 ng), analyzed by agar diffusion assay.

Data shown in Figure 12 indicated that FvPG has an enzymatic activity comparable to that of FpPG (fig 15B), but while FvPG is not inhibited by PvPGIP2 at any inhibitor amount tested, FpPG is readily inhibited with low amounts of inhibitor;

Having established that the FvPG thus purified is functional and can be used for crystallization trials, the protein eluted from the last column was collected into two different pool: the first one include fractions from 18 to 28, the second one include fractions from 29 to 34, separating the fractions that from SDS PAGE analysis have the higher concentration of protein. On the first pool was performed the crystallization trials.

3.2 Crystallization trials

X-ray crystallography is a method used for determining the atomic and molecular structure of a crystal, in which the ordered atoms present in the crystal cause a positive interference of reflected X-rays and therefore X-ray diffraction into many specific directions. By measuring the angles and intensities of these diffracted beams, it is possible to reconstruct, by indirect methods, the electron density of the molecule (or molecules) constituting the crystal and fit this density with a three-dimensional model of the molecule under examination.

The methodology of single-crystal X-ray crystallography has three basic steps. The first and often most difficult step, is to obtain adequately diffracting crystals of the material under study. The crystal should be sufficiently large (typically larger than 0.1 mm in all dimensions), pure in composition and regular in structure, with no significant internal imperfections such as cracks or twinning. The crystallization process of a molecular species in solution, can only begin when the system is in a state of supersaturation. This condition of non-equilibrium, is reached with the presence in solution of a sample at a concentration higher than the maximum expected based on its solubility constant (McPherson, A. and Weickmann, J. 1990). A situation of this type can be obtained by slow evaporation of the solvent from a saturated solution or by adding a substance that promotes precipitation.

The hanging drop vapor diffusion technique is the most popular method for the crystallization of macromolecules. In collaboration with Prof. Luca Federici (Università di Chieti), and Dr. Adele Di Matteo (CNR, Roma), I've tried to crystallize the FvPG previously purified. Since the FvPG shares a high amino acid identity with FpPG, I first tried to crystallize FvPG using the same buffer in which FpPG crystallized, as described in Federici et al., (2001), but no crystals were obtained. Therefore a complete set of new crystallization conditions were explored using commercial screens

(Crystal Screen and Crystal Screen 2 (Hampton Research); a highly effective approach to overcome the exhaustive search for suitable crystallization conditions is the use of a sparse matrix method of trial conditions that is biased and selected from known crystallization conditions for macromolecules. The formulation utilized in Crystal Screen and Crystal Screen 2 evaluates 96 unique mixtures of pH, salts, polymers and organics, and their ability to promote crystal growth. The crystallization trials were performed at two different temperatures, 4°C and 22°C, since this parameter heavily affects protein solubility;

FvPG single crystals of cubic shape were obtained from two different buffers present in the Crystals Screen: 2.4 M Sodium Malonate pH 7.0 (fig. 16 A), and in 1.8 M Ammonium citrate pH 6.8 (fig. 16 B). Both crystals were grown at 22 ° C and reached their maximum size in 5 days. The crystals were flash cooled in liquid nitrogen with no cryoprotection, and shipped to the synchrotron BeSSY in Berlin, for X-ray diffraction collection.

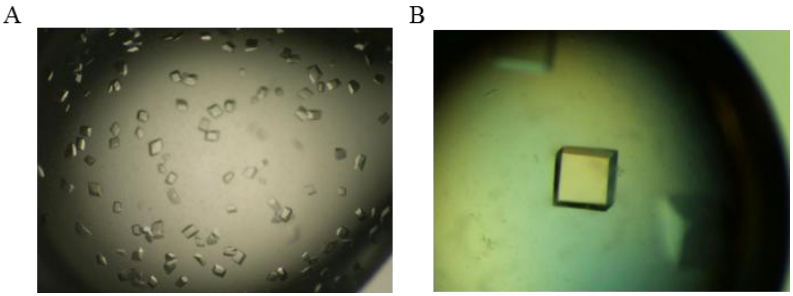

Figure 16. Crystallization trials of FvPG A) Crystals obtained in 1.8 M Ammonium citrate pH 6.8. B) Crystals obtained in 2.4 Sodium malonate pH 7.0. Both crystal were grown at 22°C.

To collect X-ray data, the crystal is exposed to an intense beam of X-rays, producing a regular pattern of diffracted beams that are registered by a CCD camera. The crystal is gradually rotated, and a different image is recorded at every orientation of the crystal. A diffraction experiment involves measuring a large number of reflection intensities. Each reflection is characterized by its amplitude and phase. However, only reflection amplitudes can be obtained from the measured intensities and no direct information about reflection phases is provided by the diffraction experiment. The so-called phase problem has therefore to be solved indirectly, for instance by comparing the Patterson functions derived from the measired intensities and from the atomic coordinates of a homologous protein in a method called Molecular replacemente. If this is succesful a set of phases is obtained and an electron density

map within the crystal may be calculated numerically by Fourier transformation of the set of observed (experimental) reflection amplitudes and their calculated phases.

These data are then combined computationally with complementary chemical information to produce and refine a model of the arrangement of atoms within the crystal. An important parameter to consider when assessing the level of confidence in a macromolecular structure is the resolution of the diffraction data utilized for its solution and refinement (often referred to as resolution of the structure). Resolution is an intrinsic characteristic of the crystal exposed to X-rays and is measured in Angstrom (Å). It can be defined as the minimum spacing (d) of crystal lattice planes that still provide measurable diffraction of X-rays. The higher the resolution, that is, the smaller the d spacing, the better, because there are more independent reflections available to define the structure.

In collaboration with Prof. Federici and Dr. Di Matteo, I've tried to solve the 3D structure of FvPG through the diffraction data collected at syncrothrone. Despite several crystals, grown in different conditions, were exposed to X-rays, the maximum resolution obtained was a 3.3 Å resolutions. This was achieved with crystals grown in 2.4 M Sodium Malone pH 7.0. This resolution is greater than the one obtained by Federici et al., (2001), to solve the 3D structure of FpPG (1.73 Å); with 3.3 Å data it is only possible to

describe the general structure of FvPG but it is not possible to accurately locate individual atoms, and therefore describe the small differences between FvPG and FpPG, which are responsible for the lack of recognition of FvPG by PvPGIP2.

3.3 Crosslinking experiments and SAXS analysis

FvPG is very similar to FpPG, with only 30 amino acid variations over 373 residues in the mature enzymes. Despite this high conservation, PvPGIP2 is unable to inhibit FvPG (Mariotti, L. et al. 2009 and data presented herein).

This lack of inhibition may be in principle either due to a lack of interaction between the two proteins or to the formation of a complex in which PG enzymatic activity is not affected. To distinguish between these two possibilities, cross-linking experiments, similar to those described in Benedetti et al., (2011) for the FpPG-PvPGIP2 complex, were performed between FvPG and PvPGIP2, using formaldehyde as crosslinker. Formaldehyde is a short cross-linker (2.3–2.7 Å), which has been used for a long time in histology and pathology to "freeze" the native state of tissues and cells (Sutherland, B. W. et al. 2008). Formaldehyde allows very fast cross-linking and stabilization of transient interactions; lower formaldehyde concentrations (0.4–2%) and especially shorter reaction times (hours)

allow the utilization of formaldehyde as a cross-linker to analyze protein-protein interactions (Vasilescu, J. et al. 2004; Schmitt-Ulms et al., 2004). The crosslinked protein was analyzed by SDS-PAGE and by SAXS analysis. SAXS is a method for the structural characterization of biological macromolecules in solution, by using ab initio and rigid body modeling (Heller, W. T. et al. 2003, Petoukhov, M. V. et al. 2013, Svergun, D. I. 1999); the 3D shapes, consistent with the pair distribution functions, can be assessed for monomeric forms, multimeric state of proteins, and protein complexes (Mertens, H. D. and Svergun, D. I. 2010, Svergun, D. I. 2010). In addition, SAXS patterns can provide structural information about flexible systems including self-aggregated systems and multidomain and intrinsically unfolded proteins (Galantini, L. et al. 2008, Hammel, M. 2012), mechanisms of denaturation and unfolding (Galantini, L. et al. 2008, Leggio, C. et al. 2008), the binding of small molecules and the stabilizing role of the ligands in denaturating conditions (Fenton, A. W. et al. 2010, Galantini, L. et al. 2010), and molecular mechanisms of ligand release (Tabarani, G. et al. 2009).

First of all, FvPG was cross-linked to PvPGIP2 with a molar ratio 1:1, in a solution containing 1% formaldehyde (see Materials and methods, section 3.4) and the reaction was incubated at 28°C for 16 h. The crosslinking reaction was also performed, under the same experimental conditions, in presence of PvPGIP2 alone (teorethical

molecular weight of 35 kDa) or FvPG alone (teorethical molecular weight of 37 kDa) to exclude the possibility that cross-linked homodimers or multimers are formed. After 16 h of incubation with formaldehyde, the three reaction solutions (FvPG, PvPGIP2 and FvPG-PvGIP2) were analyzed by SDS-PAGE and stained with Coomassie blue (fig. 17 A).

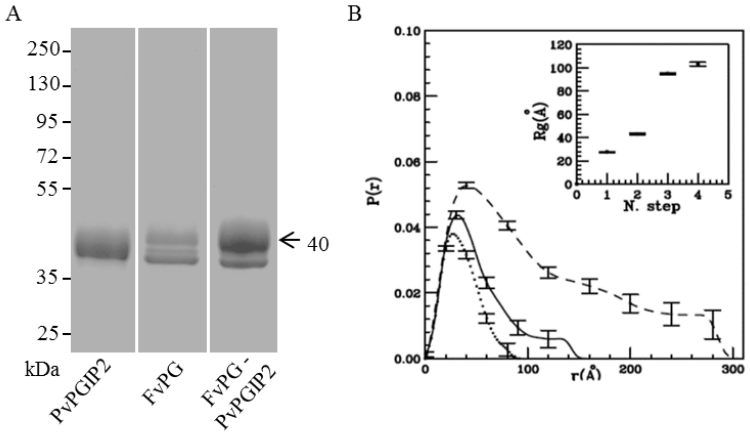

Figure 17 Analysis of the complex formed by FvPG and PvPGIP2.
A) SDS-PAGE analysis of the FvPG-PvPGIP2 cross-linked complex. The single proteins are also reported. B) Calculated pair distribution functions of the first three SAXS patterns collected for the FvPG-PvPGIP2 complex; dot-line, continuous-line and dash-line correspond to three consecutive data sets (interval times about 20 h), respectively. In the inset, the Rg values of four consecutive data sets are shown.

The single reactions do not show high molecular weight bands, indicating that the single protein (FvPG or PvPGIP2) does not cross react with itself.

Moreover the FvPG-PvPGIP2 crosslinked reaction, does not show a band at the expected molecular weight for the heterodimeric complex (fig. 17 A). It is important to emphasize that the same experiment, performed using the FpPG-PvPGIP2 couple, highlighted the presence of a band at the expected molecular weight for the heterodimeric complex (Benedetti, B. et al., 2011)

The absence of interaction between the PvPGIP2 and FvPG was also monitored by SAXS analysis of the non-crosslinked FvPG-PvPGIP2 complex. Figure 17 B shows the evolution of the p(r) functions and Rg values as a function of the time course of the experiment (with steps of 20 hours). This analysis suggests that no stable complex between the two proteins is formed, while a progressive aggregation of the sample starts after about 24 hours. It can be concluded that PvPGIP2 is unable to inhibit FvPG activity because it does not interact with this enzyme.

3.4 Loss of function mutation on FpPG

In order to identify the residues of FvPG responsible for the lack of recognition by PvPGIP2, the amino acidic variations between FpPG and FvPG were analysed. Figure 18 A reports the alignment between the FvPG and the FpPG aminoacidic sequences: in red are shown amino acidic positions where differences are found. Figure 18

B reports a surface representation of FpPG, where the amino acids contacted by PvPGIP2 (Benedetti et al., 2011) are highlighted in yellow.

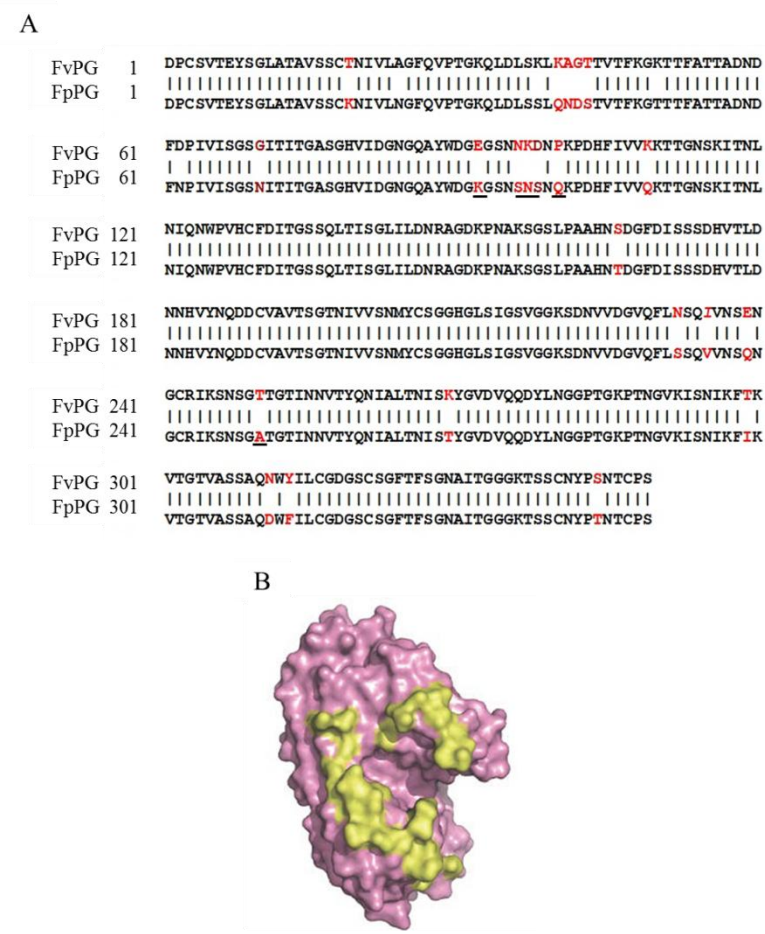

Figure 18. The FpPG amino acids contacted by PvPGIP2.
A) Alignment of FpPG and FvPG amino acid sequences. The amino acids belonging to FpPG that differ from the corresponding residues of FvPG are shown in red. Residues subjected to site-directed mutagenesis are underlined. B) Surface representation of FpPG; the amino acids contacted by PvPGIP2 are reported in yellow.

Analysis of the amino acid variations between FpPG and FvPG in the FpPG areas that are recognized by the inhibitor (fig. 18 B) indicated that main variations are located at the N-terminal edge of the active site cleft (FpPG residues S120, N121, S122 and Q124) while only one variation (FpPG residue A274) is located in the interacting area at the C-terminal edge of the active site. In a loss-of-function approach, each of these FpPG residues were mutated into the corresponding ones of FvPG, and the single mutants FpPG.S120N, FpPG.N121K, FpPG.S122D, FpPG.Q124P and FpPG.A274T, were geenrated. In addition, I've generated the triple mutant FpPG.S120N-N121K-S122D, and the variant FpPG.K116E, as a negative control. The residue at position 116 is replaced non-conservatively in FvP, is located in close proximity to the interaction area but it does not interact with PvPGIP2, according to SAXS data (Benedetti, M. et al. 2011). The singles and triple mutants were obtained by site directed mutagenesis using the QuickChange® II Site-Directed Mutagenesis Kit (Agilent) (see Materials and methods section 3.6). The primers used for the mutagenesis are listed in table II. (section Materials and Methods). To rule out the possibility that the mutations cause a variation of the PG expression levels and a possible alteration of the specific activity, western blotting analysis, on the culture filtrate of Pichia expressing the mutated PGs,

producing an equal activity on the agar diffusion assay, was performed (fig. 19).

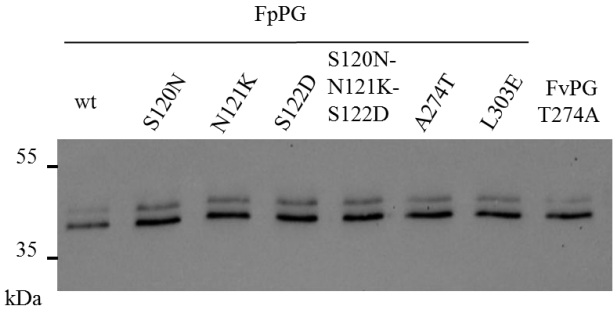

Figure 19. **Analysis of the expression of FvPG by *P. pastoris***
Western blot analysis using a polyclonal antibody against the FpPG, on the mutated and wild-type forms of FpPG and FvPG producing an equal enzymatic activity on the agar diffusion assay.

No significant effect of the mutations on the FpPG expression level was observed.

The inhibitor capability of the PvPGIP2, against the mutants, was measured with the agar diffusion assay and is reported in figure 20.

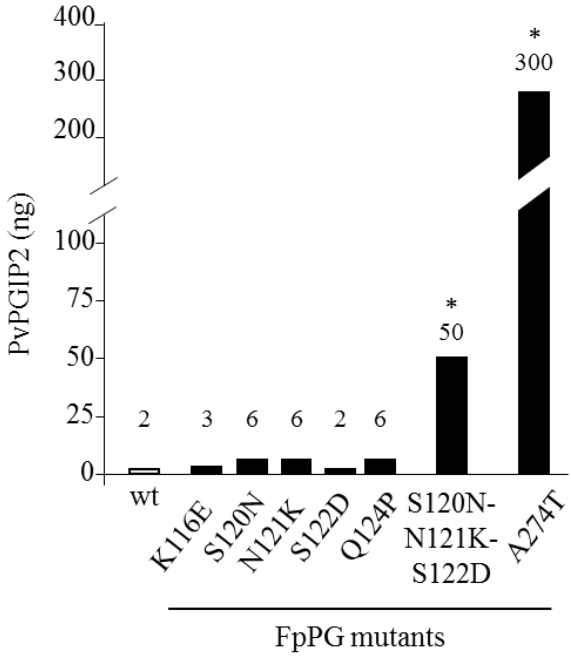

Figure 20. Inhibitory activities of PvPGIP2 against wild type (wt) and mutated forms of FpPG

The amount of PvPGIP2 (ng) causing 50% inhibition of one agarose diffusion unit of the indicated PGs at pH 4.7 are shown. Asterisks indicate statistically significant differences with wt PG, according to Student's t test (*, $P < 0.003$).

Single variations at residues S120, N121, S122 and Q124 have only a modest effect on the capability of FpPG to be inhibited by PvPGIP2 (fig. 20). Instead, the triple mutant FpPG.S120N-N121K-S122D is inhibited with a 25-fold reduced efficiency (fig. 20). The FpPG.K116E variant, chosen as a negative control, was inhibited similarly to the wild-type (fig. 20). Notably, the single mutation

A274T, caused a marked loss of inhibition by PvPGIP2 (150-fold). These data suggest that the interacting area at the C-terminal edge of the active site cleft contributes to the majority of the binding energy in the PvPGIP2-FpPG complex formation.

3.5 Gain of function mutation on FvPG

In a gain-of-function approach, I have generated by site directed mutagenesis the FvPG.T274A mutant, replacing the threonine in position 274, in the FvPG, with the alanine of the FpPG, to further confirm that this amino acid play key role in the interaction between PG and PGIP. Also for this mutant western blotting was used to confirm that the PG expression level in the culture filtrate is not affected by the mutation. The inhibitory capability of PvPGIP2 was then tested against the FvPG.T274A by agar diffusion assay and reported in the histogram in figure 21.

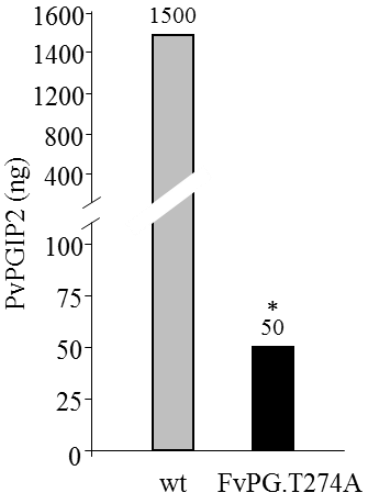

Figure 21. Inhibitory activities of PvPGIP2 against wild type (wt) and mutated forms of FvPG.

The amount of PvPGIP2 (ng) causing 50% inhibition of one agarose diffusion unit of the indicated PGs at pH 4.7 are shown. Asterisks indicate statistically significant differences with wt PG, according to Student's t test (*, $P < 0.003$).

Therefore this single mutation enables the FvPG enzyme to be recognized by PvPGIP2.

Therefore while the contribution of residues belonging to the interacting surface at the N-terminal edge of the active site is limited, albeit not negligible, it appears that a single aminoacidic position at the C-terminal edge of the recognition area acts as a switch for the PG-PGIP complex formation.

3.6 Prediction of secondary and tertiary structure of WAK1

WAK1 is a transmembrane protein, composed by an extracellular domain and an intracellular kinase domain; the extracellular domain of WAK1 contain two consensus sequence patterns for an EGF2-like domain and a calcium-binding EGF-like domain (Anderson, C. M. et al. 2001). In the N-terminal non-EGF portion of WAK1 a pectin binding domain (PDB) is present that mediates in vitro binding of OGs and structurally related alginates through five basic amino acids (R67, R91, K101,K102, R166) (Cabrera, J. C. et al. 2008, Decreux, A. et al. 2006). The entire amino acid sequence is shown in figure 22: WAK1 is composed by 735 amino acid.

```
1   MKVQEGLFLV AIFFSLACTQ LVKGQHQPGE NCQNKCGNIT IEYPFGISSG
51  CYYPGNESFS ITCKEDRPHV LSDIEVANFN HSGQLQVLLN RSSTCYDEQG
101 KKTEEDSSFT LENLSLSANN KLTAVGCNAL SLLDTFGMQN YSTACLSLCD
151 SPPEADGECN GRGCCRVDVS APLDSYTFET TSGRIKHMTS FHDFSPCTYA
201 FLVEDDKFNF SSTEDLLNLR NVMRFPVLLD WSVGNQTCEQ VGSTSICGGN
251 STCLDSTPRN GYICRCNEGF DGNPYLSAGC QDVNECTTSS TIHRHNCSDP
301 KTCRNKVGGF YCKCQSGYRL DTTTMSCKRK EFAWTTILLV TTIGFLVILL
351 GVACIQQRMK HLKDTKLREQ FFEQNGGGML TQRLSGAGPS NVDVKIFTED
401 GMKKATNGYA ESRILGQGGQ GTVYKGILPD NSIVAIKKAR LGDSSQVEQF
451 INEVLVLSQI NHRNVVKLLG CCLETEVPLL VYEFITNGTL FDHLHGSMID
501 SSLTWEHRLK IAIEVAGTLA YLHSSASIPI IHRDIKTANI LLDVNLTAKV
551 ADFGASRLIP MDKEELETMV QGTLGYLDPE YYNTGLLNEK SDVYSFGVVL
601 MELLSGQKAL CFKRPQSSKH LVSYFATATK ENRLDEIIGG EVMNEDNLKE
651 IQEAARIAAE CTRLMGEERP RMKEVAAKLE ALRVEKTKHK WSDQYPEENE
751 HLIGGHILSA QGETSSSIGY DSIKNVAILD IETGR
```

Figure 22. The entire amino acidic sequence of WAK1.
In red is reportd the signal peptide, in green the Pectin Binding Domain (PBD), in blue the first EGF-Ca^{+2} binding-like domain, in orange the second EGF like domain, in violet the transmembrane domain and in blak the Ser/Thr kinase domain. The sequence expressed in *P. pastoris* (eWAK1) is underlined.

In the amino acidic sequence of WAK1 (fig 22) are reported with different colors the different domains which can be found in the WAK1 protein: in red the signal peptide, in green the Pectin Binding Domain, in blue and orange the two EGF-Like domain, in purple the transmembrane domain and in black the Ser/Thr kinase domain. This division into functional domains, was carried out on the basis of structural prediction using the online server SWISS-MODEL (http://swissmodel.expasy.org/repository/) (fig 23).

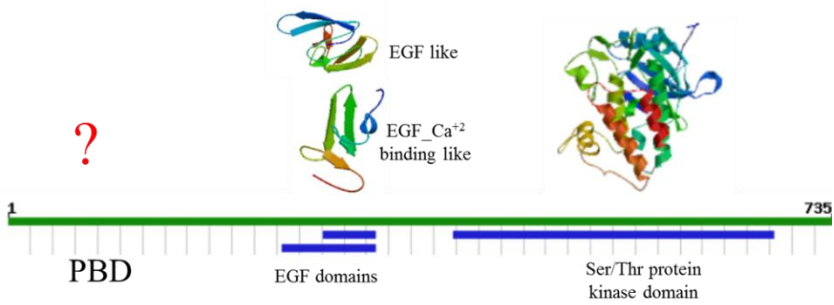

Figure 23. Prediction of tertiary structure of WAK1.
The 3D predictable structure of WAK1 was obtained using the SWISS model server (http://swissmodel.expasy.org). Only the two EGF like domains and the kinase domain have homologous protein present in the data base. The first and the last amino acid are reported (1-735). The blue line represent the portion of the protein with a predictable 3D structure; the structure find in the Protein Data Base are also reported as ribbon representation.

Only for the PBD the 3D structure is not predictable, because there are no homologous proteins in the Protein Data Bank; while 3D structure are present for the EGF-Like domains and for the Kinase domain. Since the expression in *P. pastoris* and the purification of the entire protein can be difficult and crystallographic studies on Ser/Thr like kinase domains have been extensively documented (Pereira, S. F. et al. 2011), I resorted to express and purify the isolated ectodomain of WAK1 (eWAK1), which includes the PBD and the two EGF domains.

By analyzing the amino acid sequence of eWAK1 with an on-line prediction server (NetGlyc server), based on the consensus sequence

Asn-X-Ser/Thr (where X represents any amino acid different from Proline), I've found 10 putative N-glycosylation sites (fig. 24).

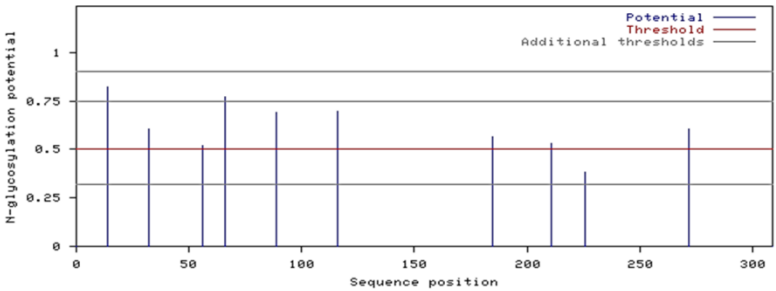

Figure 24. Prediction of N-glycosilation sites on eWAK1 amino acid sequence. Output of the server NetGlyc 1.0 indicating the position of the putative N-glycosilation sites, present in the amino acid sequence of eWAK1. The red line represent the threshold set by the program. The vertical blue lines represent the position of putative N-glycosilation sites along the eWAK1 sequence.

One of these N-glycosiltation sites does not exceed the threshold level (red line) set by the program, therefore 9 sites of the protein are potentially glycosylated in Pichia.

I also performed a prediction of the secondary structure present in eWAK1 using the on-line server GOR IV (fig 25).

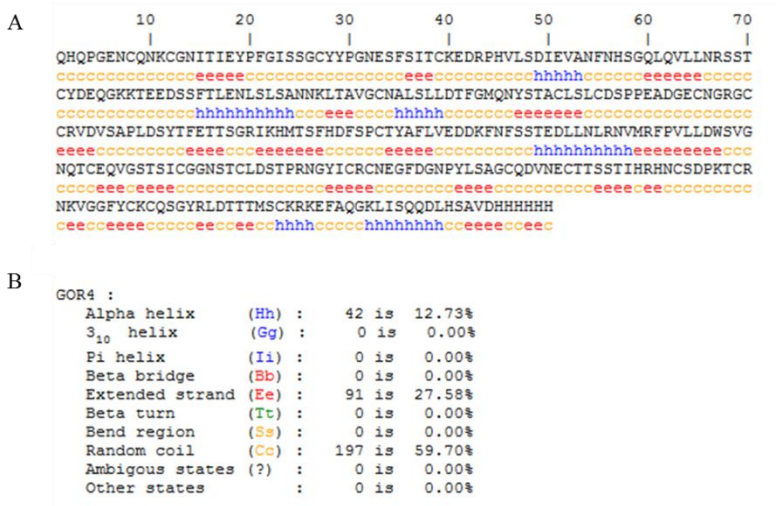

Figure 25. Prediction of the secondary structure of eWAK1 by using the online server GOR IV

A) The amino acid sequence of eWAK1: for each amino acid is indicated the type of secondary structure to which it belongs. B) The legend generated by the server GOR IV and the percentage of the secondary structure present in eWAK1.

While the server predicts that around 60% of the protein is in random coil configuration, secondary structure elements are found along its entire length with a doubled incidence of β-strands with respect to α-helices. These data suggest that the PBD is likely to be folded.

3.7 Cloning, expression and purification for crystallographic study of the extracellular domain of WAK1 (eWAK1)

For the expression of eWAK1 in *P. pastoris* I have choosen to use the pGAPZαA expression vector: this constitutive vector allows the expression of the protein in the culture medium, because the protein is fused upstream to the α-factor of *Saccharomice cerevisiae*. I have cloned into this vector the entire ectodomain including the PBD and the two EGF like domains (fig 38).
Furthermore, the protein is fused downstream to the c-*myc* epitope and to a six Histidine tag, for western blotting analysis and for making easier the purification procedure. I've amplified by PCR, using the EcorIeWAK1Fw and NotIeWAK1Rev primers, the nucleotidic sequence of eWAK1, corresponding to the amino acid sequence comprised between the amino acid 24 and the amino acid 333. The teorethical molecular weight of eWAK1 is about 37 kDa, and the isoeletric point (pI) is 5.79. The amplified and purified eWAK1 gene was cloned into the pGAPZαA vector and then, transformed in *E. coli* by electroporation. After linearization of the plasmid (according to Invitrogen manual), this was finally used to transform *P. pastoris* cells by electroporation. Several *P. pastoris* transformants were selected by PCR using EcorIeWAK1Fw and NotIeWAK1Rev as primers for the colony PCR reaction. One of

these positive transformants, was inoculated in the YPD medium and grown for 24 and 48 h. The culture filtrate was analyzed by western blotting, using an anti c-*myc* antibody (fig 26).

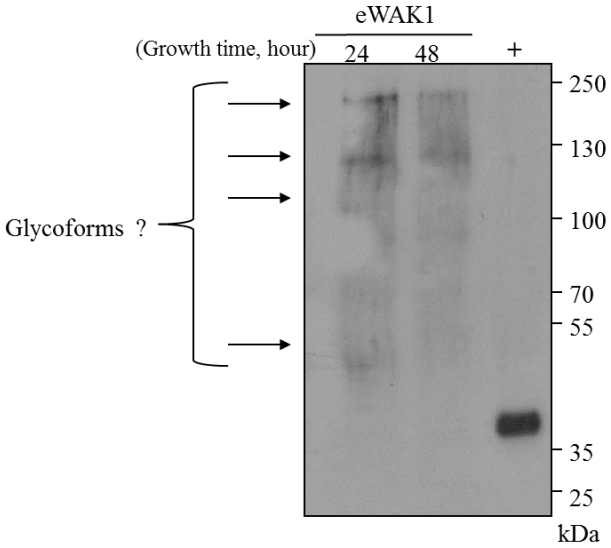

Figure 26. Western blotting analysis of the culture filtrate *P. pastoris* expressing eWAK1.

20 µL of culture filtrate was analyzed by western blotting using an antibody against the c-*myc* tag. There is no specific signal on the western blot, due probabily to the hyper-glycosilation of the protein. The black arrows indicates 4 possible glycosilated forms of eWAK1. Positive control (+), is represented by a protein tagged with c-*myc*. Theoretical molecular weight of eWAK1 is about 37 kDa.

In the western blot there is no specific signal in the lane of the culture filtrate of Pichia after 24 or 48 h of growth, but only a

smeared and faint one. This may be due to the hyper-glycosilation of eWAK1 expressed in Pichia. The black arrows (fig. 26) indicate 4 possible glycosilated forms of eWAK1. It is well known that proteins expressed in this yeast can undergo a massive N-glycosylation process (Bretthauer, R. K. and Castellino, F. J. 1999). Under this scenario, the high glycosilation of eWAK1 expressed in Pichia would affect the electrophoretic mobility in the SDS-PAGE gel, being reflected by the observed smearing.

To rule out if the expressed eWAK1 construct is highly glycosilated, I've treated the culture filtrate of Pichia expressing eWAK1, with the N-Glycosidase F (ROCHE), also known as PNGase F. This amidase cleaves between the innermost N-Acetylglucosamine and asparagine residues of high mannose, hybrid and complex oligosaccharides from *N*-linked glycoproteins. The colture filtrate of Pichia expressing eWAK1, grown for 24 and 48 h, was treated with 0.1 and 1 Unit of PNGase F for 16 h at 37°C and analyzed by western blotting.

In the western blotting showed in figure 27, the colture filtrate treated with the PNGase F showed a marked band with an apparent molecular weight of about 40 kDa.

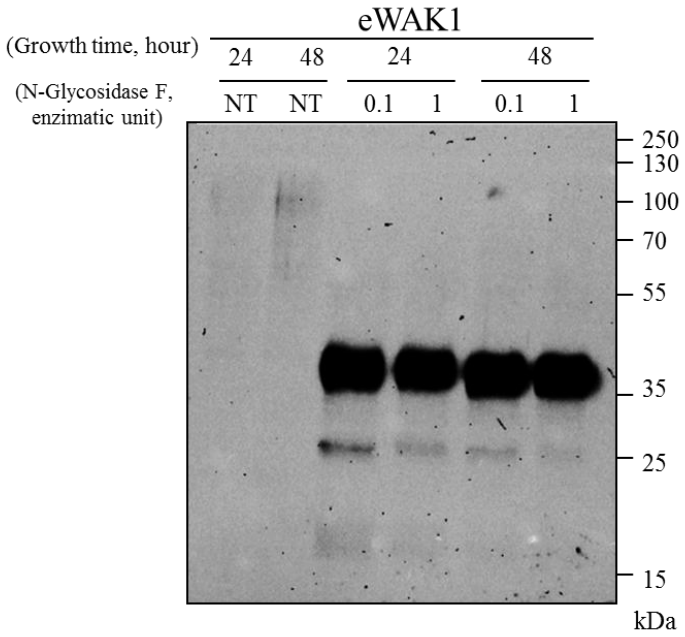

Figure 27. Western blotting analysis of the culture filtrate of *P. pastoris* expressing eWAK1.

30 µL of culture filtrate were analyzed before and after the treatment with the N-Glycosidase F, by western blotting, using an anti c-*myc* antibody There is no specific signal in the lanes indicated with NT where the colture filtrate is not treated with the enzyme; while a specific signal with an apparent molecular weight of 38 kDa appear when the colture filtrate is treated with N-glycosidase F for 16h at 37°C. Theoretical molecular weight of eWAK1 is about 37 kDa.

In the non-treated samples there is no specific signal, but only a smeared one, corroborating the hypothesis that eWAK1 expressed in Pichia is higly glycosylated. By this first analysis, the protein also

appears to be expressed in Pichia in high quantities after 24 hours. No differences are observed extending growth to 48 hours.

3.8 eWAK1 purification procedure from *Pichia pastoris*

A purification protocol to obtain a high amount of pure protein for X-ray crystallography was developed.

Initially I have tried to express the protein by growing Pichia in YPD medium. In this medium, Pichia grows very rapidly, reaching a high cellular density, which results in a high amount of protein produced. I've inoculated one colony of Pichia expressing eWAK1, in 5 ml of YPD, grown for 16 h at 28°C. After 16 h the culture was pelleted at 5000 g for 5 minutes and resuspended in 1 l of YPD and then grown for 24 h at 28°C. However, with this medium (YPD), the protein is produced in high quantities, but it is difficult to purify, because of the high amount of pigments present in the medium, that cannot be separated from the protein by anion or cation exchange chromatography (data not shown). To overcome this problem, I've tested a basal medium (BMM, see Matherials and methods for the composition) in which the amount of pigments is highly reduced. Since the BMM is a minimal medium, Pichia should grow slower than in YPD and also produce a minor amount of protein. So I compared the protein expression after 24 and 36 h of growth in YPD

and BMM, analyzing the culture filtrates by western blotting (fig. 28). In the lane of YPD (24 h), there is a marked signal, while in the lane of BMM (24h) only a faint band appears. However after 36 h of growth, in both media the expression of eWAK1 reaches a comparable level.

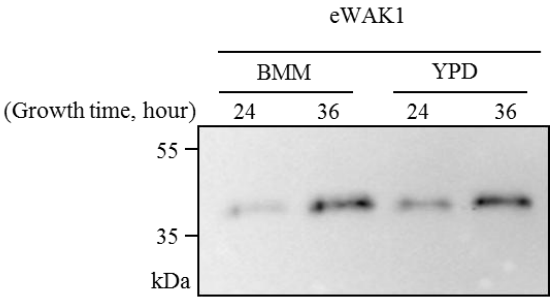

Figure 28. Western blotting analysis of the culture filtrate of *P. pastoris* expressing eWAK1.
20 µL of culture filtrate were analyzed by western blotting using an anti c-*myc* antibody *P. pastoris* where grown for the indicated time, in two different culture media: YPD, a complex medium and BMM, a basal medium. Theoretical molecular weight of eWAK1 is about 37 kDa.

Therefore I have choosen to express eWAK1 in the basal medium BMM, as this could facilitate the purification step. The Pichia transformants expressing eWAK1 was inoculated in 5 mL of YPD and growth for 16 h at 28°C; then the culture was pelleted and resuspended in 2 Lt of BMM, and grown for 36 h at 28°C. The cells were separated from the medium and the culture filtrate purified as summarized in the flow-chart in figure 29.

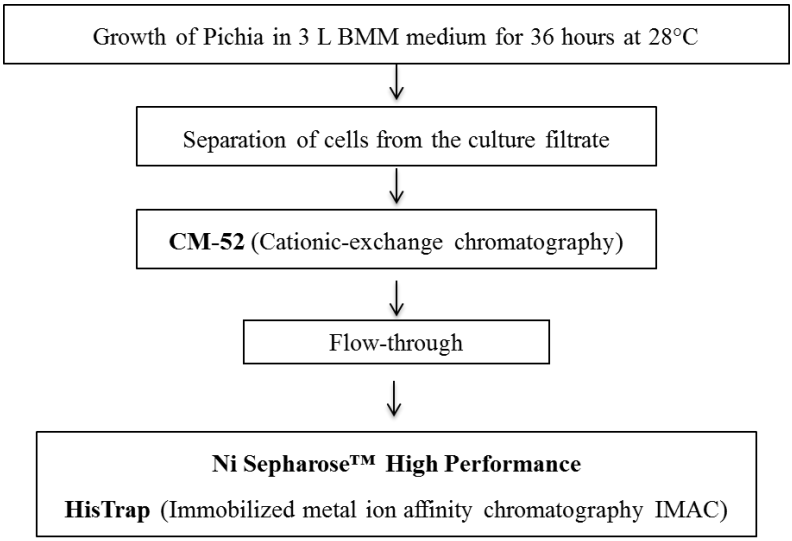

Figure 29. Flow chart of the eWAK1 purification step

The culture filtrate was loaded into a column for cation exchange chromatography (CM 52). The flow-through of this column, containing eWAK1, was collected and loaded into an affinity chromatography column (Ni Sepharose™ High Performance HisTrap GE Healthcare). The protein bound to the column through its six-Histidine tag, was eluted using a linear gradient of imidazole (from 5 mM to 500 mM); the fractions collected and pulled, were analyzed by SDS-PAGE, stained with Coomassie blue, after treatment with the PNGase F (fig. 30).

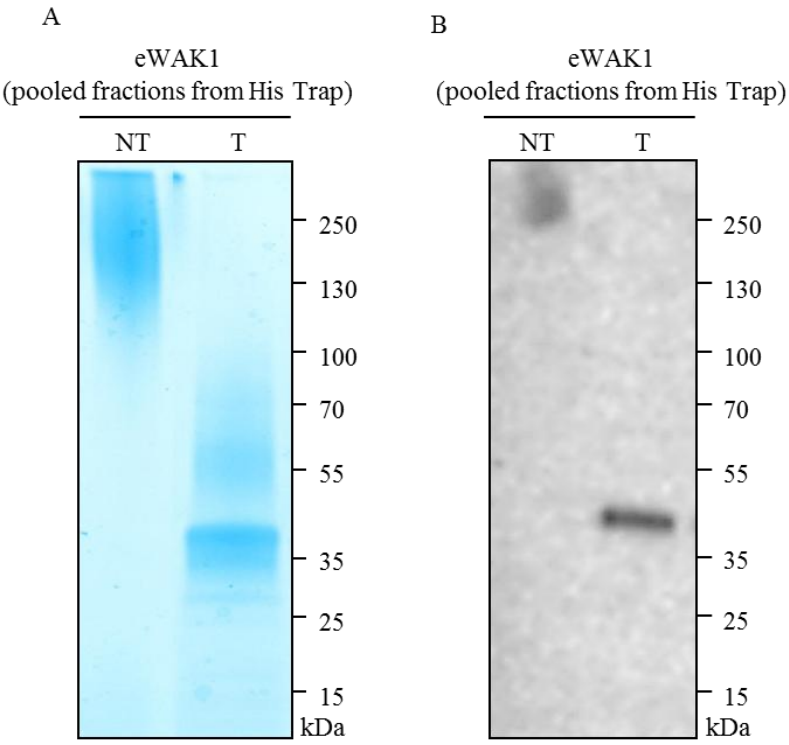

Figure 30. Analysis of the eWAK1 pooled fractions eluted from His Trap column.

SDS-PAGE (A) and Western blotting analysis (B) of pooled purifed eWAK1 (5 µL), not treated (NT) and treated (T) with 0,1 U of N-glycosidase F for 16 h at 37°C.

In the non-treated lane (NT), the signal is smeared as shown in the western blot of figure 27; after deglycosylation (lane T), a band appears at the expected molecular weight (37 kDa). In the treated lane (T), a signal related to protein degradation appears, this may be

due to the purification step or to the deglycosylation procedure. The expression level is 1.6 mg L^{-1}, and with this purification procedure, I've obtained 2 mg of eWAK1 with a good puritiy degree.

3.9 2D structure analysis of eWAK1

Before starting crystallization trials, it is necessary to carry out preliminary analysis of the purified protein, to determine whether the protein is folded in its native conformation or is in an unfolded conformation. In fact, if the protein is unfolded, it is not possible to obtain crystals (Sikder, A. R. and Zomaya, A. Y. 2005).

Circular dichroism (CD) is an important method for the investigation of protein secondary structure and structural changes during interactions with ligands, mutations and folding state (Karabencheva, T. and Christov, C. 2010). CD gives information about the unequal adsorption of left- and right-handed circularly polarized light by optically active molecules. CD bands of proteins occur in the spectral regions of far-UV or amide region (170-250 nm). This region is dominated by contributions of the peptide bonds for any given protein. The CD spectrum in this region can be analysed in terms of the content of α-helix, β-sheet, β-turn, etc. CD bands in the amide region contain information about the peptide bonds and the secondary structure of a protein and are frequently employed to

monitor changes in secondary structure in the course of structural transitions (Kelly, S. M. and Price, N. C. 1997).

Then the analysis of the CD spectrum returns the information on the secondary structure of the protein. In figure 31 is shown an example CD spectra profile of the secondary structure present in protein: a typical protein composed by α-helical has a CD spectrum represented by the solid line, with a minumun at 222 nm.

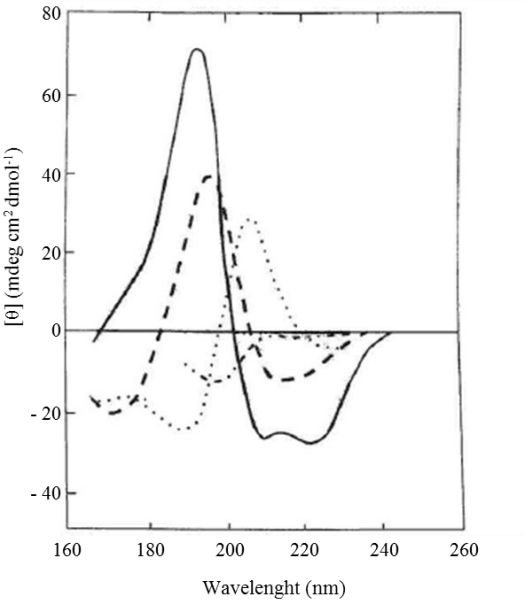

Figure 31. Representative far UV CD spectra associated with various types of secondary structure.

Solid curve, α-helix; long dashes, antiparallel β-sheet; dots, type I β -turn; dots and short dashes, irregular structure (Adapted from Kelly and Price, 2000).

A typical protein predominantly composed by β-sheets has a CD spectrum in the 200-260 nm region with a single minimum at around 215 nm. A double minima at 208 and 222 nm is instead typical of a predominantly α-helical protein. In both cases the CD signal becomes higher than zero before 200 nm, which is diagnostic of folded proteins. Conversely, if the protein is predominantly unfolded, a decreasing signal with no minima is expected in the 200-260 region, while a minimum is reached at around 190 nm (fig. 31).

Figure 32 reports the static CD spectrum obtained for eWAK1. As described above, the shape of the spectrum is consistent with the protein being predominantly unfolded.

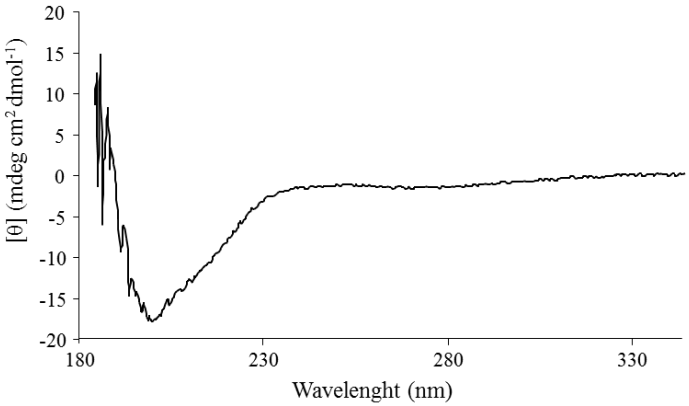

Figure 32. Circular dichroism analysis.
The CD spectra of purified eWAK1 (15 μM) in a 1-mm pathlength quartz cuvette.

3.10 3D structure analysis of eWAK1

To further confirm the finding that eWAK1 is expressed and purified from Pichia as an unfolded protein, I have measured the intrinsic fluorescence of eWAK1, during a denaturation process. Fluorescence refers to the emission of radiation from the excited electronic state of a molecule that has been populated by absorption. The absorption of proteins in the 250-300 nm range is determined by the aromatic side chains of Phe, Tyr, and Trp (YANARI, S. and BOVEY, F. A. 1960). The absorption spectra of the aromatic amino acids depend on the nature of the molecular neighbourhood of the respective chromophores, resulting in shifts in wavelength: a red shift of the spectrum is observed when the polarity of the solvent decreases and *vice versa* (Royer, C. A. 2006)(Royer et al., 2006). In folded native proteins, aromatic residues are in general buried within the hydrophobic core of the molecule; when they become exposed to the aqueous solvent during unfolding, they give rise to a decrease in absorbance in the 285–295 nm region.

Changes in protein conformation, such as unfolding, very often lead to large changes in fluorescence emission (Royer, C. A. 2006). Both the intensity and wavelength of maximum emission are sensitive measures of the polarity of the tryptophan environment, and hence provide useful information about tertiary structure.

I've measured the intrinsic fluorescence of eWAK1, recorded between 300 and 400 nm, with an excitation wavelength of 280 nm, in presence of increasing amounts of urea (fig.33) (0 M to 5.6 M- see Materials and Methods section 3.11).

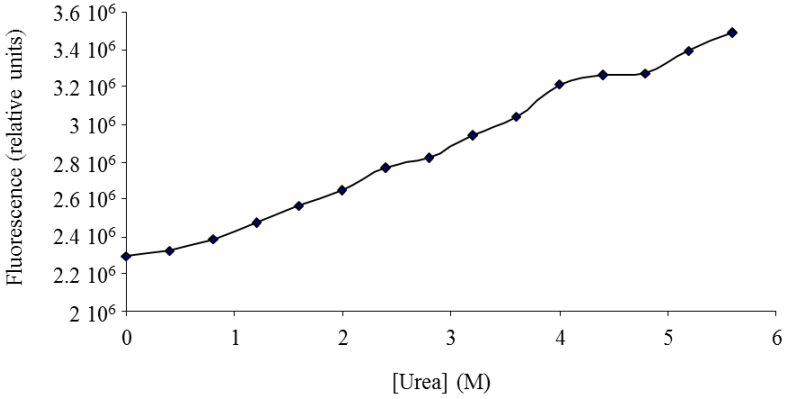

Figure 33. Equilibrium unfolding of eWAK1 monitored by intrinsic fluorescence.

The urea-induced denaturation, measured at pH 7.5 in 50 mM Tris HCl, 150 mM NaCl and 10°C, was followed by fluorescence at different wavelengths (5 µM protein concentration). The line represents the best fit between four different wavelenghts; but there is no evidence of a two-state model, indicating that eWAK1 is unfolded.

Figure 33 shows the fluorescence signal as a function of urea concentration. While a modest, continuous, increase of fluorescence is observed as urea concentration increases, there is no evidence for a

sigmoidal cooperative transition, or a combination of sigmoidal transitions, that is typical of folded proteins in moving to the unfolded state in a two state model or in more complex scenarios involving the presence of intermediates.

Therefore chemical denaturation data, followed by intrinsic triptophan fluorescence, are in agreement with the analysis of CD spectra, and suggest that the eWAK1 construct expressed in Pichia is unstructured. This is likely due to the high glycosilation of the protein, which may interfere with the proper folding equilibrium of the domain. Alternatively, and in contrast with predictions, the PBD might be natively unfolded with its signal predominating over the EGF-like domains one, in both CD and fluorescence experiments. Even if this event is unlikely, it cannot be ruled out unless the protein is expressed in a native fashion in a different heterologous system.

3.11 eWAK1-HA, transient expression in *Nicotiana tabacum* mediated by *Agrobacterium tumefaciens*

Next, I decided to express the eWAK1 protein in plant, to overcome the problem of high glycosylation in *Pichia.* Transient expression in plant, mediated by *Agrobacterium tumefaciens,* allows in many cases the rapid production of large amounts of recombinant protein (Pogue, G. P. et al. 2010, Sheludko, Y. V. 2008).

Transient expression in plant was achieved using *A. tumefaciens* [strain GV3101] transformed with plant expression binary vectors pB7m34GW-eWAK1HA (Gateway system™). eWAK1 is fused upstream to the 35 S promoter, and downstream to the Human influenza hemagglutinin epitope (HA).

To obtain this vector I've amplified by PCR, using the primers FwattB1eWAK1 and RevattB2eWAK1, the entire nucleotidic sequence of eWAK1 including the signal peptide, using the eWAK1 cDNA as template. Then using the Gateway system™ kit (see Matherials and methods section 3.12) I've introduced in the pDONR/221 Zeo vector the entire sequence of eWAK1. The pENTRY-eWAK1 vector was cloned into *E. coli*, extracted and purified and, by a recombination reaction between the pENTRY-eWAK1 vector, the two other vectors that contain the 35S promoter and the HA epitope coding sequence (pEN-R2-F-L3 and pEN-R2-3XHA-L3 respectively) and the pB7m34GW vector, I've obtained the final expression vector for eWAK1 in plant. The 35S::eWAK1-HA vector was cloned into *Agrobacterium tumefaciens*. Adult leaves of *Nicotiana tabacum* cv. Petit Havana SR1 4 (weeks old) were agroinfiltrated with *A. tumefaciens*, transformed with 35S::eWAK1-HA construct; 3 days post-infiltration, I extracted, from transformed tissue, the total proteins and analyzed them by western blotting, using an anti-HA antibody. As already known, He et al., (1996)

succeeded to extract the entire endogenous WAK1 from *A.thaliana* adult leaves only in denaturating conditions, by using 4% SDS, 50 mM DTT and boiling the sample fot three minutes. This extraction condition is very denaturant for any protein. Therefore, I first used the same procedure described by He et al. (1996) only to assess whether eWAK1-HA was transiently expressed in plant after Agroinfiltration. Leaf tissues were ground in the Resuspension buffer (see Materials and Methods section 3.13), than the sample was centrifugated to separate the pellet and supernatant fractions. The pellet fraction is enriched with cell wall components, and eWAK1-HA should be found in these fractions rather than in the supernatant. The two fractions were treated with Extraction buffer (4% SDS and 50 mM DTT) and then boiled. In the immunoblot, shown in figure 34 there is no specific signal in the extracts from leaf infiltrated with *A. tumefaciens* transformed with an empty vector, both in the pellet and supernatant fraction.

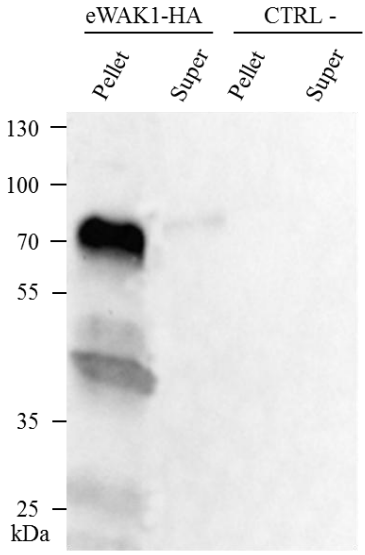

Figure 34. Western blotting analysis of leaf tissue expressing eWAK1-HA. Total protein (60 ug) from *N. tabacum* leaves, that transiently express eWAK1-HA, were analyzed by Western blotting, using an anti-HA antibody (SIGMA). Tissue were ground as described in He *et al.*,1996. As negative control (CTRL-) was used the whole extract from leaves infiltrated with *A. tumefaciens* transformed with an empty vector. Theoretical molecular weight of eWAK1 fused to the HA is about 40 kDa.

Conversely, in the tissue infiltrated with eWAK1-HA, an intense band appears with an apparent molecular weight of 70 kDa in the pellet fraction, and a faint band, of the same molecular weight, in the supernatant fraction. The shift in the molecular weight from 40 kDa (theoretical molecular weight of eWAK1 fused to the HA), to 70 kDa, may be due again to the glycosylation present on the protein.

These experiments demonstrate that eWAK1 may be expressed in *N. tabacum* to reasonably high levels.

However, the harsh treatment used so far likely denaturates the protein. Therefore I've tried to extract the eWAK1-HA, transiently expressed in *N. tabacum*, with non-denaturant buffer. Agroinfiltrated tissue was treated with different buffers that could not interfere with the folding of the protein: the buffer used previously (4% SDS, 50 mM DTT and 50 mM Tris-Hcl pH 6.8) and shown in the western blot with the number 1 (fig. 35); the same buffer without DTT (2); a buffer composed only by Tris-HCl and DTT (3), and a buffer composed only by Tris-HCl (NT).

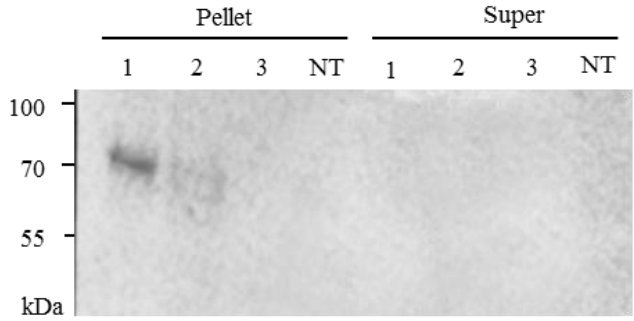

Figure 35. Western blotting analysis of leaf tissue expressing eWAK1-HA
Total protein (60 ug) extracts from *N. tabacum* leaves, that transiently express the eWAK1-HA construct, were analysed by using an anti-HA monoclonal antibody (SIGMA). Tissue were ground in the Resuspension buffer, than centrifuged at 18000 x *g*, to separate pellet and supernatant and treated separately with: (1) 50 mM Tris HCl pH 6.8, 50 mM DTT, 4% (v/v) SDS; (2) Tris HCl pH 6.8 and 4% (v/v) SDS; (3) Tris HCl pH 6.8 and 50 mM DTT. A band, with an apparent weight of 100 kDa, appear only when tissue were treated with 4 % SDS and 50 mM DTT. Non treated (NT) samples were only ground in the Resusoension buffer.

Figure 35 shows that only if the pellet fractions are treated at the same time with 4% SDS, 50 mM DTT and Tris-HCl, it is possible to extract eWAK-HA from the leaves. Future efforts should therefore be directed to finding suitable mild conditions for extracting eWAK1 from Agroinfiltrated leaves, without affecting protein folding.

4. DISCUSSION

The PG-PGIP interaction is paradigmatic for studying the key recognition events that underlie plant immunity (Misas-Villamil, J. C. et al., 2008). In this study I have taken under consideration the PGIP2 from *Phaseolus vulgaris* (PvPGIP2) and the PG expressed by *Fusarium verticillioides* (FvPG). PvPGIP2 is the best characterized inhibitor and has the strongest inhibitory activity against most of the tested PG from different pathogens (Borras-Hidalgo, O. et al., 2012; D'Ovidio, R. et al., 2004). Interestingly, the FvPG enzyme is not inhibited by any known PGIP, including PvPGIP2 (Mariotti, L et al., 2009). Therefore, understanding the structural basis underlying the capacity of FvPG to escape inhibition by PvPGIP2 may shed additional light on this crucial interaction for plant immunity and also contribute to design of improved inhibitors for crop protection.

The interaction between FvPG and PvPGIP2 was studied using different approaches, wich required large amounts of proteins. To this purpose, FvPG was expressed in *P. pastoris* and purified by means of different chromatographic techniques: the protein obtained was functional and characterized by two glycoforms, as the FpPG expressed and purified in *P. pastoris* (Federici, L. et al. 2001). The expression level of FvPG is 15 mg/L, and the purification yield is about 5 mg: this quantity allowed to perform different experiments, first of all X-Ray crystallography studies. The purified protein, as described in section 3.1, has a purity degree greater than 90 %,

suitable for crystallization trials, by the hangind drop vapour diffusion techniques. I have obtained crystals of cubic shape in 2.4 Sodium malonate pH 7; but the diffraction data collected from these crystals had a low resolution, which did not allow to characterize the small differences between FvPG and FpPG that permit FvPG to escape from the recognition of PvPGIP2. However the combination of SAXS structural data, sequence analysis and mutational data enabled us to analyze the behavior of the FvPG enzyme that, despite being 92.5 % identical to FpPG, is not inhibited by PvPGIP2, as well as by any other known PGIP.

First I demonstrated that the lack of inhibition is due to the PvPGIP2 failure to form a complex with FvPG (see figure 16). Through SAXS analysis between FvPG and PvPGIP2, I have showed that the FvPG does not form a complex with PvPGIP2, under the same experimental conditions where a complex with other PG isozymes, including FpPG, is readily stabilized. Then I analyzed the differences at the two areas of FpPG that are recognized by PvPGIP2. The ^{120}SNSNQ^{124} loop located at the N-terminal side of the active site cleft of FpPG is replaced in FvPG by a loop of sequence ^{120}NKDNP^{124}, with just one residue conserved out of five. Instead, the C-terminal interacting area is well conserved and just the A274T single amino-acidic variation is observed. In a loss of function approach, I mutated residues of FpPG into the corresponding ones of

FvPG. Contrary to our expectations, single site mutations at the ^{120}SNSNQ^{124} loop had only a modest effect on the inhibitory capability of PvPGIP2 (see figure 19). Conversely, the mutation of FpPG A274 into the corresponding threonine of FvPG resulted in a remarkable 150-fold decrease of PvPGIP2 inhibition efficiency.

Since the FpPG A274 residue faces F80 and Y105 in PvPGIP2 its mutation to threonine may add steric hindrance or cause a loss of hydrophobic stabilizing interactions. Interestingly, the PvPGIP2 Y105 residue was previously shown to be subjected to positive selection for the interaction (Casasoli, M. et al. 2009).

These findings suggest that the residue at position 274 acts as a molecular switch that allows FvPG to escape recognition by PvPGIP2. To support this hypothesis, in a gain of function approach, I mutated the FvPG T274 into the corresponding alanine of FpPG and observed, remarkably, that this single mutation is sufficient to confer to this enzyme the capability of being inhibited by PvPGIP2 (see figure 20). Therefore, the residue occupying this topological position in the PG structure appears to play a key role in the interaction.

This perfectly fits with an arms race scenario where PGs evolve to escape recognition by PGIPs while, on the opposite side, PGIPs evolve to enhance their inhibition spectra. In the future we aim at exploiting the knowledge gained about the PG-PGIP interaction to

develop *in vitro* PGIP variants that are able to inhibit PGs that are currently escaping recognition.

The OGs released by the degradation of pectin, due to the action of PGs, are perceived by their receptor, WAK1, and elicit several defense responses in plants (Brutus, A. et al. 2010; De Lorenzo et al., 2011). The binding between OGs and WAK1 has not yet been characterized at the structural level, because the 3D structure of this protein is not yet been solved by X-Ray crystallography. The ectodomain has no similarity with known structures, particularly in the region deputed to bind OGs, the PBD (Pectin Binding Domain). The aim of this part of my thesis was to verify if it is possible to produce high quantities of purified eWAK1 domain for X-ray crystallography, a technique that is heavily dependent on the availability of high sample amounts for crystallization conditions screening. First I have expressed the entire ectodomain of WAK1 (eWAK1) in the yeast *Pichia pastoris*. For the expression in the yeast, I have used the pGAPZαA vector that allow the secretion of the expressed protein in the culture medium, to facilitate the purification procedure. *P. pastoris* expresses eWAK1 in high amounts, but the protein was found to be highly glycosylated (see section 3.7). The glycosylation impaired the detection of the protein

on the western blot, unless the protein was enzymatically deglycosylated.

Nevertheless, an efficient purification protocol was developed that allowed to obtain the protein construct in quantities suitable for structural studies. However, preliminary structural analysis, through circular dichroism, suggested that the protein is unstructured (see figure 33). This result was also confirmed by chemical denaturation experiments, followed by intrinsic triptophan fluorescence. This is likely due to the high and non-natural glycosilation of the protein expressed in the heterologous yeast Pichia, which may interfere with the proper folding equilibrium.

To overcome this problem a different expression system was chosen, i.e. the transient expression of eWAK1 in *Nicotiana tabacum*. For this case, I have used the recombinant Gateway system (Invitrogen): the protein is fused upstream to the 35S promoter and downstream to the HA epitope; then the vector obtained after two steps of recombination, is cloned into *Agrobacterioum tumefaciens* and adult tobacco leaves (4 weeks old), agroinfiltrated. Proteins were extracted using a denaturant buffer (4 % SDS, 50 mM DTT and 50 mM Tris-HCl) previously developed by He et al. (1996) to extract endogenous WAK1 from *Arabidopsis thaliana*. This procedure allowed demonstrating that eWAK1-HA is transiently expressed in tobacco leaves. Interestingly, a single band was observed in western blots, at

a higher molecular weight than the expected one for the protein alone but without the use of any deglycosilation agent. This suggests that, while glycosilation is also present in the construct expressed in planta, this is likely to be more specific and less extended than the hyper glycosilation obtained in Pichia. Since the buffer used for extracting the protein from tobacco leaves likely denaturates the protein, future efforts will be done to develop a procedure that allows the extraction of a natively folded protein product from tobacco leaves.

Alternatively, we will try to express eWAK1 in Arabidopsis protoplasts which, due to the absence of a plant cell wall, may facilitate protein purification.

5. MATERIALS AND METHODS

5.1 FpPG and FvPG Expression and Purification

The polygalacturonase of *Fusarium phyllophilum* (FpPG) was expressed and purified as previously described (Benedetti, M. et al. 2011). The cDNA encoding the polygalacturonase of *Fusarium verticillioides* (FvPG) strain 62264 was cloned in pGAPZαA (Invitrogen) (fig. 36) using the EcoRI and XbaI restriction sites introduced by using the primers FvPGEcoFw and FvPGXbaRv (Table I).

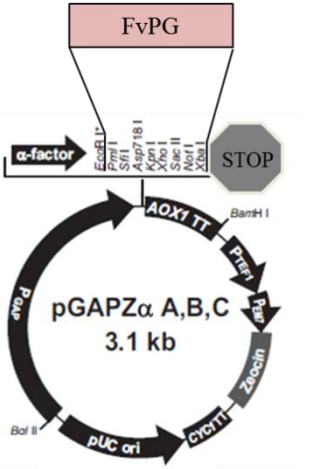

Figure 36. Vector used for expression of FvPG in *P. pastoris.*
FvPG was cloned in frame with the signal sequence for secretion of the yeast (*Saccharomyces cerevisiae*) α factor. The restriction sites (EcoRI and Not I) are highlighted.

The construct, generated in frame with the signal sequence for secretion of the yeast (*Saccharomyces cerevisiae*) α factor, was

amplified by transforming *Escherichia coli* TOP10F competent cells (Invitrogen). pGAPZαA-FvPG was extracted from the cells using a plasmid mini prep kit (Qiagen) and analyzed by digestion with EcoRI and XbaI restriction enzymes, followed by 1% (w/v) agarose gel analysis. The plasmid DNA was linearized with AvrII restriction enzyme and used to transform *Pichia pastoris* X33 cells (Invitrogen) by electroporation. The selection of the zeocin-resistant *P. pastoris* transformants was carried out according to the manufacturer's instruction (Invitrogen). The medium used for growth of *P. pastoris* contained 1% (w/v) yeast extract, 1% (w/v) tryptone and 2% (w/v) glucose. The filtrate obtained from 3-days-old culture was concentrated using a Vivaflow 200 (Sartorius Stedim) and dialyzed against 20 mM Sodium Acetate (NaOAc) pH 4.0. The dialyzed sample was loaded on a diethylaminoethyl cellulose resin (DEAE, Whatman) pre-equilibrated with 20 mM NaOAc pH 4.0. The flow through was then loaded on a HiTrap SP-Sepharose column (GE Healthcare), pre5 equilibrated with 20 mM NaOAc pH 4.0. Eluition was carried out using a linear gradient of NaCl (from 0 to 1 M) in the same buffer. The fractions that showed the highest PG activity were pooled and dialyzed against 20 mM NaOAc pH 4.0. Subsequently, ammonium sulfate was added to the dialyzed proteins to reach 2 M final concentration and the sample was loaded on a HiTrap Phenyl-Sepharose column (GE Healthcare) pre-equilibrated with 20 mM

NaOAc pH 4.0 and ammonium sulphate 2 M. Elution was performed by decreasing the concentration of ammonium sulphate (from 2 M to 0 M in 10 min) in 20 mM NaOAc pH 4.6. Purified fractions as determined by SDS-PAGE were pooled.

5.2 PvPGIP2 Expression and Purification

The PG-inhibiting protein 2 of *Phaseolus vulgaris* pv Pinto (PvPGIP2) was cloned in pGAPZαA (Invitrogen), expressed in *Pichia pastoris* X33 (Invitrogen) and purified as previously described.

5.3 Crystallography

Crystallization was performed at 22°C using the hanging-drop vapour-diffusion technique (fig 37). Crystals were obtained by mixing 1 µl protein solution with an equal volume of reservoir solution and equilibrating against 500 µl reservoir solution. Initial crystallization trials were carried out using commercial crystallization screens (Crystal Screen and Crystal Screen 2; Hampton Research). I have obtained cubic crystals both in a solution consisting of 2.4 M Sodium malonate pH 7.0, and in one containing 1.8 M Ammonium citrate pH 6.8. The crystal was mounted on a

nylon loop and flash-cooled in a nitrogen-liquid at 100 K. Crystals were not cryoprotected.

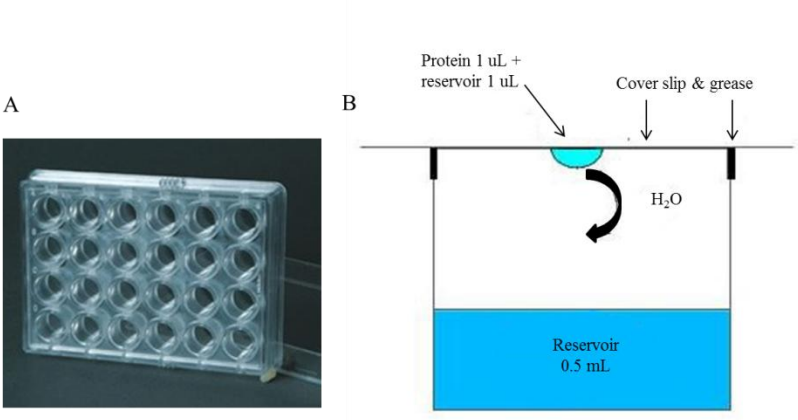

Figure 37. Hanging drop vapour diffusion.
A) A plate used for the Hangig drop methods, for crystals grown. B) Schematic representation of a crystallization experiment with the technique of hanging drop. A small amount of a crystallization solution is put into a small reservoir. A drop of protein solution and a drop of crystallization solution are placed onto the sitting drop post in the chamber. The chamber is sealed to start the crystallization process.

FvPG complete data were collected to 3.3 Å resolution at the BL14-1 beamline of the BeSSY Synchrotron (Berlin, Germany). The crystals belong to the centered tetragonal space group $I4_122$, with unit-cell parameters a=b= 193.31 Å, c= 197.56 Å and α=β=γ= 90. A total of 540 frames of data were collected with 0.5° oscillation range. All intensity data were indexed, integrated and scaled with the HKL-2000 package (Otwinowski, Z. and Minor, W. 1997). The FvPG structure was determined by molecular replacement using the

program MOLREP (Vagin, A. and Teplyakov, A. 2000) and the FpPG protein as a template for Patterson calculations (pdb code: 1hg8; (Federici, L. et al. 2001).

5.4 FvPG-PvPGIP2 Chemical Cross-Linking

The crosslinking reaction between PvPGIP2 and FvPG was performed as previously described. Seventy micrograms of PvPGIP2 were cross-linked to 78 μg of FvPG (molar ratio 1:1) in 200 μL of a solution containing 50 mM NaOAc pH 4.6 supplied with fresh 1% methanolfree formaldehyde (Thermo-Fisher Scientific). The reaction was incubated at 28°C for 16 h and finally concentrated to 2 μg of total proteins/mL. The single proteins used as negative control were cross linked using the same reaction conditions. Cross-linked proteins and negative controls were analyzed by SDS-PAGE.

5.5 SAXS data acquisition and analysis

SAXS measurements were carried at 25.0°C in a quartz capillary of 1 mm diameter by using a Kratky Compact camera (Anton Paar), with a slit collimation system and equipped with a NaI scintillation counter. The nickel-filtered copper Ka radiation (λ = 1.5418 Å) was used and scattering curves were recorded within the

range of $0.01 \leq q \leq 0.4$ $Å^{-1}$ ($q = 4\pi\sin\theta/\lambda$, where 2θ is the scattering angle). The intensity of the primary beam was measured by employing the moving slit method. The collimated scattering intensities were put on an absolute scale, corrected for the solvent and the capillary contributions, and expressed in electron units eu (electrons2 $Å^{-3}$) per centimetre primary beam length (Kratky, O. et al. 1973, Pilz, I. et al. 1979) One eu corresponds to 7.94056 x10-2 cm^{-1} in terms of total scattering cross section of a particles ensemble (Orthaber, D. and Glatter, O. 1998). Spectra were interpreted by the Indirect Fourier transform method as implemented in the ITP program (Laggner, P. et al. 1977). For very dilute samples (no particle interactions) the scattered intensity, I(q), can be related to the pair distribution function p(r) of the single scattering particle according to the equation:

$$I(q) = \int_0^\infty p(r)\frac{\sin(qr)}{qr}dr$$

On the basis of this equation, the ITP extracts of the p(r) function from the desmeared scattering pattern. The p(r) function is strongly dependent on the shape and size of the scattering particles and vanishes at the maximum particle size Dmax. Furthermore, it permits the determination of the electronic radius of gyration Rg. (Laggner, P. et al. 1977). The obtained values are more accurate than those derived from the Guinier approximation (Svergun, D. I. 2010).

Absolute intensity values reliability and instrumental set up correcteness were checked determining the mass, the gyration radius and the p(r) function of defatted Human Serum Albumin in solution at pH 7.4 (Leggio, C. et al. 2008). The resolution limit allows analyzing particles with a maximum dimension of 310 Å. Each SAXS measurement was obtained averaging three consecutive runs. The superimposition of the patterns allowed to exclude the formation of oligomers or a damage of the sample due to the X-ray radiation exposure. In the FvPG-PGIP2 complex, aggregation was detected after 24 hours.

5.6 Site Directed Mutagenesis

FvPG genes cloned in the pGAPZαA vector, were used as templates for site directed mutagenesis using the QuickChange® II Site-Directed Mutagenesis Kit (Agilent) according to the manufacturer's instructions. The forward and reverse primers used to introduce the mutations in the corresponding positions of *FpPG* (L303E, K310T, S363K, K116E, S120N, N121K, S122D, Q124P and S120N-N121K-S122D), *FvPG* (T274A and L303E) are listed in Table II. The mutated genes were sequenced to confirm the presence of the desired mutations and subsequently used to transform *P. pastoris*, as heterologous expression system as described above.

5.7 Agar diffusion assay

The capability of wild-type PvPGIPs to inhibit the activity of the native and variant forms of FpPG, and FvPG was measured by the agar diffusion assay as previously described [20]. PG activity was expressed as agarose diffusion units and one unit was defined as the amount of enzyme that produced a halo of 0.5 cm radius (external to the inoculation well) after 16 h at 30°C. The agarose inhibition unit was defined as the amount of PvPGIP2 causing 50% inhibition of 1 agarose diffusion unit at pH 4.7.

5.8 eWAK1, Expression and purification in the heterologous system *Pichia pastoris*

The ectodomain of WAK1 (AGI code: AT1G21250, corresponding to the amino acid sequence between the amino acid 24 and amino acid 333) was cloned in pGAPZαA (Invitrogen) using the EcoRI and NotI restriction sites introduced by using the primers EcorIeWAK1Fw and NotIeWAK1Rev (Table I).

The construct was generated in frame with the signal sequence for secretion of the yeast (*Saccharomyces cerevisiae*) α factor, and with the c-*myc* and His tags sequence, for the detection on western blotting analysis (fig. 38); pGAPZαA-eWAK1 was amplified by transforming *Escherichia coli* TOP10F competent cells (Invitrogen)

and extracted from the cells using a plasmid mini prep kit (Qiagen) and analyzed by digestion with EcoRI and NotI restriction enzymes, followed by 1% (w/v) agarose gel analysis. The plasmid DNA was linearized with AvrII restriction enzyme and used to transform *Pichia pastoris* X33 cells (Invitrogen) by electroporation. The selection of the zeocin-resistant *P. pastoris* transformants was carried out according to the manufacturer's instruction (Invitrogen).

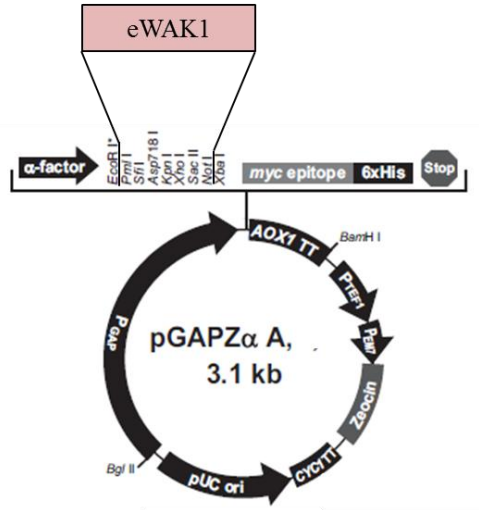

Figure 38. Vector used for expression of eWAK1 in *P. pastoris.*
eWAK1 (from 24 to 333 amino acid) was cloned in frame with the signal sequence for secretion of the yeast (*Saccharomyces cerevisiae*) α factor, and with the c-*myc* and His tags sequence. The restriction sites (EcoRI and Not I) are highlighted are highlighted.

The medium used for growth of *P. pastoris* contained 1,3% (w/v) Yest Nitrogen Base (SIGMA), 3% (w/v) glucose and 100 mM sodium phosphate buffer pH 6. The filtrate obtained from 2-days-old culture was loaded on a carboxymethyl cellulose resin (CM52, Whatman) pre-equilibrated with 20 mM NaOAc pH 4.6. The flow through was then loaded on a HiTrap Q-Sepharose column (GE Healthcare), pre equilibrated with 20 mM NaOAc pH 4.6. Eluition was carried out using a linear gradient of NaCl (from 0 to 1 M) in the same buffer. The fractions were analyzed by SDS-PAGE and western blotting, using an anti c-*myc* antibody 9E10 (Santa Cruz Biotechnology, inc.); the fraction thaht showed the highest signal on western blotting, were loaded on a His Trap HP Sepharose column (GE Healthcare) pre-equilibrated with 20 mM sodium phosphate buffer pH 7, 0,3 M NaCl and 15 mM imidazole. Elution was performed by increasing the concentration of imidazole (from 15 mM to 1M) in the same buffer. Purified fractions as determined by SDS-PAGE were pooled.

5.9 Deglycosilation of eWAK1 expressed in *P. pastoris*

Upon purification, 20 μg of protein samples were treated with 0,1 U/μL of N-Glycosidase F (ROCHE) in 50 ul of deglycosiltion buffer (250 mM Potassium phosphate buffer pH 8.0,

50 mM EDTA and 1% (v/v) 2-mercaptoethanol), incubated at 37°C overnight.

5.10 Circular Dichroism (CD)

CD spectra of eWAK1 were recorded between 260 and 190 nm at a concentration of 15 μM using a Jasco spectropolarimeter J710 (Jasco, Inc., Easton, MD) and a 1-mm pathlength quartz cuvette (Hellma, Plainview, NY).

5.11 Fluorescence

Fluorescence emission spectra of eWAK1 were recorded between 300 and 400 nm with an excitation wavelength of 280 nm at a protein concentration of 5 μM, using a Fluoromax spectrofluorimeter (Jobin Yvon, New Jersey), in a 1 × 0.4 cm quartz cuvette (Hellma). Chemical denaturation, increasing urea concentration in the sample (from 0 M to 5.6 M), was followed recording the emission at 340, 350, 360 and 370 nm. The buffer used was 20 mM sodium phosphate buffer pH 7 and 0.3 M NaCl.

5.12 eWAK1 transient expression *Nicotiana tabacum*

Constructs for expression of the entire ectodomain of WAK1 (amino acid 1 to amino acid 333) in *planta* was obtained by using the Multisite Gateway Recombination Cloning Technology (Life Technologies); eWAK1 was cloned in frame with the the 3xHA tag. In particular pEN-eWAK1 entry clones was generated in the pDONR221/Zeo vector (Life Technologies). Primer used are FwattB1eWAK1 and RevattB2eWAK1, and are listed in table I. Subsequently, for eWAK1 constructs, multisite recombination was performed by using the pEN-R2-F-L3 and pEN-R2-3XHA-L3 vectors, which contain the 35S promoter and the 3xHA coding sequence tag respectively, and pB7m34GW as destination binary vector that confers the phosphinothricin resistance for the selection of mutant. All Gateway compatible vectors were previously described (Karimi, M. et al. 2002) and obtained from Plant System Biology (Ghent University; http://gateway.psb.ugent.be/).

Agrobacterium tumefaciens [GV3101] was transformed with the plasmids obtained above, and grown on LB plates (5 g yeast extract, 10 g tryptone, 5 g NaCl, 1ml 1M NaOH in 1l) containing rifampicin (150µg/ml), gentamycin, (50µg/ml), and spectinomycin (100µg/ml). Colonies were inoculated in 5 ml liquid cultures of LB containing antibiotics (see above) and grown under constant shaking of 180 rpm and 28˚C for 16–24h. A 2 ml aliquot of the cell cultures was

harvested by centrifugation and resuspended in 2 mL of YEB medium (per liter: 5 g of beef extract, 1 g of yeast extract, 5 g of sucrose, and 0.5 g of $MgSO_4 \cdot 7H_2O$), supplemented with antibiotics. The bacterial culture was incubated at 28°C with agitation until reaching the stationary growth phase. One milliliter of culture was transferred into an Eppendorf tube, and the bacteria were pelleted by centrifugation at 2200g for 5 min in a microcentrifuge at room temperature. The pellet was washed twice with 1 mL of the infiltration buffer (IF) (50 mM Mes, pH 5.6, 2 mM Na3PO4, 0.5% glucose [w/v], and 100 mM acetosyringone [Aldrich]) and then resuspended in 1 mL of the same buffer. The bacterial suspension was diluted with infiltration buffer to adjust the inoculum concentration to the stated final OD600. The inoculum was delivered to the lamina tissues of tobacco leaves by gentle pressure infiltration through the stomata of the lower epidermis, by using a 1-mL syringe without a needle. The infected area of the leaf was delimited and labeled with an indelible pen, and the plant was incubated at 21°C, 16/8h light/dark (Brandizzi, F. et al. 2002).

5.13 eWAK1-HA: Protein Extraction, Gel Electrophoresis, and Immunoblot Analysis

Plant tissue samples were ground in the Resuspension buffer (50 mM MES pH 5.6, 2 µM PMSF and Protease Inhibitor Cocktail [SIGMA P9599] 1:100). The samples were centrifuged at 18000 x *g*, to separate pellet and supernatant, than treated separately with Extraction buffer (Tris HCl pH 6.8, 50 mM DTT, 4% (v/v) SDS) and boiled for 3 minutes as described in (He, Z. H. et al. 1996). The denatured samples were fractionated in 10% SDS-polyacrylamide gel electrophoresis and electroblotted to nitrocellulose using the Trans-Blot® Turbo™ Transfer System (BIO RAD).

The content of total proteins was determined by the Bradford method (Bradford MM, 1976). Expression HA-fused proteins, was analyzed by Western blotting, anti-HA (SIGMA) antibody, and revealed using ECL kit (Amersham). Chemio-luminescence was detected by Chemidoc (BIORAD).

Table II Primers used in this study**.**

Primers name	Sequence
FvPGEcoFw	ACCTGAGAATTCGATCCCTGCTCCGTGAC
FvPGXbaRv	GCCTATCTAGACTAGCTGGGGCAAGTGTT
FwFpK116E	CAGGCGTACTGGGATGGCGAAGGTTCTAACAGCAATAGC
RvFpK116E	GCTATTGCTGTTAGAACCTTCGCCATCCCAGTACGCCTG
FwFpS120N	GGATGGCAAAGGTTCTAACAACAATAGCAACCAAAAGCCCG
RvFpS120N	CGGGCTTTTGGTTGCTATTGTTGTTAGAACCTTTGCCATCC
FwFpN121K	GGCAAAGGTTCTAACAGCAAGAGCAACCAAAAGCCCGATC
RvFpN121K	GATCGGGCTTTTGGTTGCTCTTGCTGTTAGAACCTTTGCC
FwFpS122D	GGCAAAGGTTCTAACAGCAATGACAACCAAAAGCCCGATCAC
RvFpS122D	GTGATCGGGCTTTTGGTTGTCATTGCTGTTAGAACCTTTGCC
FwFpQ124P	GTTCTAACAGCAATAGCAACCCAAAGCCCGATCACTTCATCG
RvFpQ124P	CGATGAAGTGATCGGGCTTTGGGTTGCTATTGCTGTTAGAAC
FwFpA274T	GCATCAAGTCCAACTCTGGCACAACTGGCACGATCAACAACG
RvFpA274T	CGTTGTTGATCGTGCCAGTTGTGCCAGAGTTGGACTTGATGC
FwFpS120N-N121K	GGGATGGCAAAGGTTCTAACAACAAGGACAACCAAAAGCCCGATCAC
RvFpS120N-N121K	GTGATCGGGCTTTTGGTTGTCCTTGTTGTTAGAACCTTTGCCATCCC
FwFvT274A	GCATCAAGTCCAACTCTGGAGCAACTGGCACGATCAACAACG
RvFvT274A	CGTTGTTGATCGTGCCAGTTGCTCCAGAGTTGGACTTGATGC
FwattB1eWAK1	GGGGACAAGTTTGTACAAAAAAGCAGGCTTAATGAAGGTGCAGGAGGGTTT
RevattB2eWAK1	GGGGACCACTTTGTACAAGAAAGCTGGGTATGCAAACTCTTTACGCTTGCA
EcorIeWAK1Fw	CAGGACGAATTCCAACATCAACCTGGTGAGAAT
NotIeWAK1Rev	GGTGCTGCGGCCGCTGCAAACTCTTTACGCTTGCA

6. REFERENCE LIST

Aguero,C.B., Uratsu,S.L., Greve,C., Powell,A.L.T., Labavitch,J.M., Meredith,C.P., and Dandekar,A.M. (2005) Evaluation of tolerance to Pierce's disease and *Botrytis* in transgenic plants of *Vitis vinifera* L. expressing the pear PGIP gene. Mol.Plant Pathol. 6:43-51.

Allen,R.L. and Lonsdale,D.M. (1993) Molecular characterization of one of the maize polygalacturonase gene family members which are expressed during late pollen development. Plant J. 3:261-271.

Altamura,M.M., Zaghi,D., Salvi,G., De Lorenzo,G., and Bellincampi,D. (1998) Oligogalacturonides stimulate pericycle cell wall thickening and cell divisions leading to stoma formation in tobacco leaf explants. Planta 204:429-436.

Anderson,C.M., Wagner,T.A., Perret,M., He,Z.H., He,D., and Kohorn,B.D. (2001) WAKs: cell wall-associated kinases linking the cytoplasm to the extracellular matrix. Plant Mol.Biol. 47:197-206.

Asiegbu,F.O., Daniel,G., and Johansson,M. (1994) Defense-related reactions of seedling roots of Norway spruce to infection by *Heterobasidion annosum* (Fr.) Bref. Physiol.Mol.Plant Pathol. 45:1-19.

Aziz,A., Heyraud,A., and Lambert,B. (2004) Oligogalacturonide signal transduction, induction of defense-related responses and protection of grapevine against Botrytis cinerea. Planta 218:767-774.

Baydoun,E.A.H. and Fry,S.C. (1985) The immobility of pectic substances in injured tomato leaves and its bearing on the identity of the wound hormone. Planta 165:269-276.

Beck,M., Zhou,J., Faulkner,C., MacLean,D., and Robatzek,S. (2012) Spatio-temporal cellular dynamics of the Arabidopsis flagellin receptor reveal activation status-dependent endosomal sorting. Plant Cell 24:4205-4219.

Bellincampi,D., Cardarelli,M., Zaghi,D., Serino,G., Salvi,G., Gatz,C., Cervone,F., Altamura,M.M., Costantino,P., and De Lorenzo,G. (1996) Oligogalacturonides prevent rhizogenesis in *rol B* transformed tobacco explants by inhibiting auxin-induced expression of the *rol B* gene. Plant Cell 8:477-487.

Bellincampi,D., Dipierro,N., Salvi,G., Cervone,F., and De Lorenzo,G. (2000) Extracellular H_2O_2 induced by oligogalacturonides is not involved in the inhibition of the auxin-regulated *rolB* gene expression in tobacco leaf explants. Plant Physiol. 122:1379-1385.

Bellincampi,D., Salvi,G., De Lorenzo,G., Cervone,F., Marfà,V., Eberhard,S., Darvill,A., and Albersheim,P. (1993) Oligogalacturonides inhibit the formation of roots on tobacco explants. Plant J. 4:207-213.

Benedetti,M., Leggio,C., Federici,L., De Lorenzo,G., Pavel,N.V., and Cervone,F. (2011) Structural Resolution of the Complex between a Fungal Polygalacturonase and a Plant Polygalacturonase-Inhibiting Protein by Small-Angle X-Ray Scattering. Plant Physiol. 157:599-607.

Benen,J.A.E., Kester,H.C., and Visser,J. (1999) Kinetic characterization of *Aspergillus niger* N400 endopolygalacturonases I, II and C. Eur.J.Biochem. 259:577-585.

Bent,A.F. and Mackey,D. (2007) Elicitors, effectors, and R genes: the new paradigm and a lifetime supply of questions. Annu.Rev.Phytopathol. 45:399-436.

Bergey,D.R. and Ryan,C.A. (1999) Wound- and systemin-inducible calmodulin gene expression in tomato leaves. Plant Mol.Biol. 40:815-823.

Bianchi,M.E. (2007) DAMPs, PAMPs and alarmins: all we need to know about danger. J.Leukoc.Biol. 81:1-5.

Bishop,P.D. and Ryan,C.A. (1987) Plant-cell wall polysaccharides that activate natural plant defenses (review). Meth.Enzymol. 138:715-724.

Boller,T. and Felix,G. (2009) A renaissance of elicitors: perception of microbe-associated molecular patterns and danger signals by pattern-recognition receptors. Annu.Rev.Plant Biol. 60:379-406.

Bonnin,E., Le Goff,A., Korner,R., Vigouroux,J., Roepstorff,P., and Thibault,J.F. (2002) Hydrolysis of pectins with different degrees and patterns of methylation by the endopolygalacturonase of *Fusarium moniliforme*. Biochim.Biophys.Acta 1596:83-94.

Braccini,I. and Perez,S. (2001) Molecular basis of ca(2+)-induced gelation in alginates and pectins: the egg-box model revisited. Biomacromolecules. 2:1089-1096.

Branca,C., De Lorenzo,G., and Cervone,F. (1988) Competitive inhibition of the auxin-induced elongation by a-D-oligogalacturonides in pea stem segments. Physiol.Plant. 72:499-504.

Brandizzi,F., Snapp,E.L., Roberts,A.G., Lippincott-Schwartz,J., and Hawes,C. (2002) Membrane protein transport between the endoplasmic reticulum and the Golgi in tobacco leaves is energy

dependent but cytoskeleton independent: evidence from selective photobleaching. Plant Cell 14:1293-1309.

Bretthauer,R.K. and Castellino,F.J. (1999) Glycosylation of Pichia pastoris-derived proteins. Biotechnol.Appl.Biochem. 30 (Pt 3):193-200.

Broekaert,W.F. and Peumans,W.J. (1988) Pectic polysaccharides elicit chitinase accumulation in tobacco. Physiol.Plant. 74:740-744.

Brutus,A., Sicilia,F., Macone,A., Cervone,F., and De Lorenzo,G. (2010) A domain swap approach reveals a role of the plant wall-associated kinase 1 (WAK1) as a receptor of oligogalacturonides. Proc.Natl.Acad.Sci.USA 107:9452-9457.

Cabrera,J.C., Boland,A., Messiaen,J., Cambier,P., and Van Cutsem,P. (2008) Egg box conformation of oligogalacturonides: the time-dependent stabilization of the elicitor-active conformation increases its biological activity. Glycobiology 18:473-482.

Cantu,D., Vicente,A.R., Labavitch,J.M., Bennett,A.B., and Powell,A.L. (2008) Strangers in the matrix: plant cell walls and pathogen susceptibility. Trends Plant Sci. 13:610-617.

Caprari,C., Mattei,B., Basile,M.L., Salvi,G., Crescenzi,V., De Lorenzo,G., and Cervone,F. (1996) Mutagenesis of

endopolygalacturonase from *Fusarium moniliforme*: Histidine residue 234 is critical for enzymatic and macerating activities and not for binding to polygalacturonase-inhibiting protein (PGIP). Mol.Plant-Microbe Interact. 9:617-624.

Casasoli,M., Federici,L., Spinelli,F., Di Matteo,A., Vella,N., Scaloni,F., Fernandez-Recio,J., Cervone,F., and De Lorenzo,G. (2009) Integration of evolutionary and desolvation energy analysis identifies functional sites in a plant immunity protein. Proc.Natl.Acad.Sci.USA 106:7666-7671.

Cervone,F., De Lorenzo,G., Salvi,G., Bergmann,C., Hahn,M.G., Ito,Y., Darvill,A., and Albersheim,P. (1989) Release of phytoalexin elicitor-active oligogalacturonides by microbial pectic enzymes. In Signal Molecules in Plants and Plant-Microbe Interactions. NATO ASI Series, Volume H36, B.J.J.Lugtenberg, ed (Heidelberg, FRG: Springer Verlag), pp. 85-89.

Chinchilla,D., Boller,T., and Robatzek,S. (2007a) Flagellin signalling in plant immunity. Current Topics in Innate Immunity 598:358-371.

Chinchilla,D., Shan,L., He,P., De Vries,S., and Kemmerling,B. (2009) One for all: the receptor-associated kinase BAK1. Trends Plant Sci 14:535-541.

Chinchilla,D., Zipfel,C., Robatzek,S., Kemmerling,B., Nurnberger,T., Jones,J.D., Felix,G., and Boller,T. (2007b) A flagellin-induced complex of the receptor FLS2 and BAK1 initiates plant defence. Nature 448:497-500.

Chisholm,S.T., Coaker,G., Day,B., and Staskawicz,B.J. (2006) Host-microbe interactions: shaping the evolution of the plant immune response. Cell 124:803-814.

Choi,S.W., Tamaki,T., Ebine,K., Uemura,T., Ueda,T., and Nakano,A. (2013) RABA members act in distinct steps of subcellular trafficking of the Flagellin Sensing2 receptor. Plant Cell 25:1174-1187.

Cote,F. and Hahn,M.G. (1994) Oligosaccharins: structures and signal transduction. Plant Mol.Biol. 26:1379-1411.

D'Ovidio,R., Raiola,A., Capodicasa,C., Devoto,A., Pontiggia,D., Roberti,S., Galletti,R., Conti,E., O'Sullivan,D., and De Lorenzo,G. (2004) Characterization of the complex locus of bean encoding polygalacturonase-inhibiting proteins reveals subfunctionalization for defense against fungi and insects. Plant Physiol. 135:2424-2435.

Davies,H.A., Daniels,M.J., and Dow,J.M. (1997) Induction of extracellular matrix glycoproteins in Brassica petioles by wounding

and in response to *Xanthomonas campestris*. Mol.Plant-Microbe Interact. 10:812-820.

Davis,D.A. and Currier,W.W. (1986) The effect of the phytoalexin elicitors, arachidonic and eicosapentaenoic acids, and other unsaturated fatty acids on potato tuber protoplasts. Physiol.Mol.Plant Pathol. 28:431-441.

Davis,G.L. and Hunter,E. (1987) A charged amino acid substitution within the transmembrane anchor of the Rous Sarcoma virus envelope glycoprotein affects surface expression but not intracellular transport. J.Cell Biol. 105:1191-1203.

de las Heras,A., Patiño,B., Posada,M.L., Martinez,M.J., Vazquez,C., and Jaen,M.T.G. (2003) Characterization and in vitro expression patterns of an exopolygalacturonase encoding gene from *Fusarium oxysporum* f.sp. *radicis lycopersici*. Journal of Applied Microbiology 94:856-864.

De Lorenzo,G. (1994) La poligalatturonasi, la PGIP e gli oligogalatturonidi nella comunicazione tra piante e funghi fitopatogeni. Giornale Botanico Italiano 128:507-519.

De Lorenzo,G., Brutus,A., Savatin,D.V., Sicilia,F., and Cervone,F. (2011) Engineering plant resistance by constructing chimeric

receptors that recognize damage-associated molecular patterns (DAMPs). FEBS Lett. 585:1521-1528.

De Lorenzo,G., Cervone,F., Bellincampi,D., Caprari,C., Clark,A.J., Desiderio,A., Devoto,A., Forrest,R., Leckie,F., Nuss,L., and Salvi,G. (1994) Polygalacturonase, PGIP and oligogalacturonides in cell-cell communication. Biochem.Soc.Trans. 22:396-399.

De Lorenzo,G., D'Ovidio,R., and Cervone,F. (2001) The role of polygacturonase-inhibiting proteins (PGIPs) in defense against pathogenic fungi. Annu.Rev.Phytopathol. 39:313-335.

De Lorenzo,G. and Ferrari,S. (2002) Polygalacturonase-inhibiting proteins in defense against phytopathogenic fungi. Curr.Opin.Plant Biol. 5:295-299.

Decreux,A. and Messiaen,J. (2005) Wall-associated kinase WAK1 interacts with cell wall pectins in a calcium-induced conformation. Plant Cell Physiol. 46:268-278.

Decreux,A., Thomas,A., Spies,B., Brasseur,R., Van Cutsem,P., and Messiaen,J. (2006) In vitro characterization of the homogalacturonan-binding domain of the wall-associated kinase WAK1 using site-directed mutagenesis. Phytochemistry 67:1068-1079.

Denoux,C., Galletti,R., Mammarella,N., Gopalan,S., Werck,D., De Lorenzo,G., Ferrari,S., Ausubel,F.M., and Dewdney,J. (2008) Activation of defense response pathways by OGs and Flg22 elicitors in Arabidopsis seedlings. Mol Plant 1:423-445.

Desjardins,A.E. and Hohn,T.M. (1997) Mycotoxins in plant pathogenesis. Mol.Plant-Microbe Interact. 10:147-152.

Desjardins,A.E., Maragos,C.M., and Proctor,R.H. (2006) Maize ear rot and moniliformin contamination by cryptic species of *Fusarium subglutinans*. Journal of Agricultural and Food Chemistry 54:7383-7390.

Desjardins,A.E., Plattner,R.D., and Proctor,R.H. (1996) Genetic and biochemical aspects of fumonisin production. Adv.Exp.Med.Biol. 392:165-173.

Di Matteo,A., Bonivento,D., Tsernoglou,D., Federici,L., and Cervone,F. (2006) Polygalacturonase-inhibiting protein (PGIP) in plant defence: a structural view. Phytochemistry 67:528-533.

Di Matteo,A., Federici,L., Mattei,B., Salvi,G., Johnson,K.A., Savino,C., De Lorenzo,G., Tsernoglou,D., and Cervone,F. (2003) The crystal structure of PGIP (polygalacturonase-inhibiting protein),

a leucine-rich repeat protein involved in plant defense. Proc.Natl.Acad.Sci.USA 100:10124-10128.

English,P.D., Maglothin,A., Keegstra,K., and Albersheim,P. (1972) A cell wall-degrading endopolygalacturonase secreted by *Colletotrichum lindemuthianum*. Plant Physiol. 49:293-297.

Evdokimov,A.G., Anderson,D.E., Routzahn,K.M., and Waugh,D.S. (2001) Unusual molecular architecture of the Yersinia pestis cytotoxin YopM: a leucine-rich repeat protein with the shortest repeating unit. J.Mol.Biol. 312:807-821.

Federici,L., Caprari,C., Mattei,B., Savino,C., Di Matteo,A., De Lorenzo,G., Cervone,F., and Tsernoglou,D. (2001) Structural requirements of endopolygalacturonase for the interaction with PGIP (polygalacturonase-inhibiting protein). Proc.Natl.Acad.Sci.USA 98:13425-13430.

Federici,L., Di Matteo,A., Fernandez-Recio,J., Tsernoglou,D., and Cervone,F. (2006) Polygalacturonase inhibiting proteins: players in plant innate immunity? Trends Plant Sci. 11:65-70.

Federici,L., Mattei,B., Caprari,C., Savino,C., Cervone,F., and Tsernoglou,D. (1999) Crystallization and preliminary X-ray diffraction study of the endo- polygalacturonase from *Fusarium*

moniliforme. Acta Crystallogr.D.Biol.Crystallogr. 55 (Pt 7):1359-1361.

Felix,G., Duran,J.D., Volko,S., and Boller,T. (1999) Plants have a sensitive perception system for the most conserved domain of bacterial flagellin. Plant J. 18:265-276.

Fenton,A.W., Williams,R., and Trewhella,J. (2010) Changes in small-angle X-ray scattering parameters observed upon binding of ligand to rabbit muscle pyruvate kinase are not correlated with allosteric transitions. Biochemistry 49:7202-7209.

Ferrari,S., Galletti,R., Denoux,C., De Lorenzo,G., Ausubel,F.M., and Dewdney,J. (2007) Resistance to *Botrytis cinerea* induced in Arabidopsis by elicitors is independent of salicylic acid, ethylene, or jasmonate signaling but requires PHYTOALEXIN DEFICIENT3. Plant Physiol. 144:367-379.

Ferrari,S., Galletti,R., Vairo,D., Cervone,F., and De Lorenzo,G. (2006) Antisense expression of the *Arabidopsis thaliana AtPGIP1* gene reduces polygalacturonase-inhibiting protein accumulation and enhances susceptibility to *Botrytis cinerea*. Mol.Plant Microbe Interact. 19:931-936.

Ferrari,S., Plotnikova,J.M., De Lorenzo,G., and Ausubel,F. (2003a) Arabidopsis local resistance to *Botrytis cinerea* involves salicylic acid and camalexin and requires EDS4 and PAD2, but not SID2, EDS5 or PAD4. Plant J. 35:193-205.

Ferrari,S., Savatin,D.V., Sicilia,F., Gramegna,G., Cervone,F., and Lorenzo,G.D. (2013) Oligogalacturonides: plant damage-associated molecular patterns and regulators of growth and development. Front Plant Sci. 4:49.

Ferrari,S., Vairo,D., Ausubel,F.M., Cervone,F., and De Lorenzo,G. (2003b) Tandemly duplicated Arabidopsis genes that encode polygalacturonase-inhibiting proteins are regulated coordinately by different signal transduction pathways in response to fungal infection. Plant Cell 15:93-106.

Frediani,M., Cremonini,R., Salvi,G., Caprari,C., Desiderio,A., D'Ovidio,R., Cervone,F., and De Lorenzo,G. (1993) Cytological localization of the *pgip* genes in the embryo suspensor cells of *Phaseolus vulgaris* L. Theor.Appl.Genet. 87:369-373.

Futamura,N., Mori,H., Kouchi,H., and Shinohara,K. (2000) Male flower-specific expression of genes for polygalacturonase, pectin methylesterase and beta-1,3-glucanase in a dioecious willow (*Salix gilgiana* Seemen). Plant Cell Physiol. 41:16-26.

Galantini,L., Leggio,C., Konarev,P.V., and Pavel,N.V. (2010) Human serum albumin binding ibuprofen: a 3D description of the unfolding pathway in urea. Biophys.Chem. 147:111-122.

Galantini,L., Leggio,C., and Pavel,N.V. (2008) Human serum albumin unfolding: a small-angle X-ray scattering and light scattering study. J.Phys.Chem.B 112:15460-15469.

Galletti,R., De Lorenzo,G., and Ferrari,S. (2009) Host-derived signals activate plant innate immunity. Plant Signal.Behav. 4:33-34.

Galletti,R., Denoux,C., Gambetta,S., Dewdney,J., Ausubel,F.M., De Lorenzo,G., and Ferrari,S. (2008) The AtrbohD-mediated oxidative burst elicited by oligogalacturonides in Arabidopsis is dispensable for the activation of defense responses effective against *Botrytis cinerea*. Plant Physiol. 148:1695-1706.

Garcia-Maceira,F.I., Di Pietro,A., Huertas-Gonzalez,M.D., Ruiz-Roldan,M.C., and Roncero,M.I. (2001) Molecular characterization of an endopolygalacturonase from Fusarium oxysporum expressed during early stages of infection. Appl.Environ.Microbiol. 67:2191-2196.

Gassmann,W. and Bhattacharjee,S. (2012) Effector-triggered immunity signaling: from gene-for-gene pathways to protein-protein interaction networks. Mol.Plant Microbe Interact. 25:862-868.

Gibeaut,D.M. and Carpita,N.C. (1993) Synthesis of (1-->3), (1-->4)-b-D-glucan in the Golgi apparatus of maize coleoptiles. Proc.Natl.Acad.Sci.USA 90:3850-3854.

Goehre,V., Spallek,T., Haeweker,H., Mersmann,S., Mentzel,T., Boller,T., de Torres,M., Mansfield,J.W., and Robatzek,S. (2008) Plant Pattern-Recognition Receptor FLS2 Is Directed for Degradation by the Bacterial Ubiquitin Ligase AvrPtoB. Curr.Biol. 18:1824-1832.

Gou,X., He,K., Yang,H., Yuan,T., Lin,H., Clouse,S.D., and Li,J. (2010) Genome-wide cloning and sequence analysis of leucine-rich repeat receptor-like protein kinase genes in *Arabidopsis thaliana*. BMC Genomics 11:19.

Hahn,M.G., Darvill,A.G., and Albersheim,P. (1981) Host-pathogen interactions. XIX. The endogenous elicitor, a fragment of a plant cell wall polysaccharide that elicits phytoalexin accumulation in soybeans. Plant Physiol. 68:1161-1169.

Hammel,M. (2012) Validation of macromolecular flexibility in solution by small-angle X-ray scattering (SAXS). Eur.Biophys.J. 41:789-799.

He,Z.H., Cheeseman,I., He,D.Z., and Kohorn,B.D. (1999) A cluster of five cell wall-associated receptor kinase genes, *Wak1-5*, are expressed in specific organs of *Arabidopsis*. Plant Mol.Biol. 39:1189-1196.

He,Z.H., Fujiki,M., and Kohorn,B.D. (1996) A cell wall-associated, receptor-like protein kinase. J.Biol.Chem. 271:19789-19793.

He,Z.H., He,D.Z., and Kohorn,B.D. (1998) Requirement for the induced expression of a cell wall associated receptor kinase for survival during the pathogen response. Plant J. 14:55-63.

Heese,A., Hann,D.R., Gimenez-Ibanez,S., Jones,A.M., He,K., Li,J., Schroeder,J.I., Peck,S.C., and Rathjen,J.P. (2007) The receptor-like kinase SERK3/BAK1 is a central regulator of innate immunity in plants. Proc.Natl.Acad.Sci.USA 104:12217-12222.

Heller,W.T., Krueger,J.K., and Trewhella,J. (2003) Further insights into calmodulin-myosin light chain kinase interaction from solution scattering and shape restoration. Biochemistry 42:10579-10588.

Hind,S.R., Malinowski,R., Yalamanchili,R., and Stratmann,J.W. (2010) Tissue-type specific systemin perception and the elusive systemin receptor. Plant Signal.Behav. 5:42-44.

Huang,Q. and Allen,C. (1997) An exo-poly-alpha-D-galacturonosidase, PehB, is required for wildtype virulence of Ralstonia solanacearum. J Bacter 179:7369-7378.

Huffaker,A. and Ryan,C.A. (2007) Endogenous peptide defense signals in Arabidopsis differentially amplify signaling for the innate immune response. Proc.Natl.Acad.Sci.USA 104:10732-10736.

Jenczmionka,N.J. and Schafer,W. (2005) The Gpmk1 MAP kinase of *Fusarium graminearum* regulates the induction of specific secreted enzymes. Curr.Genet. 47:29-36.

Jiang,D., Liang,J., and Noble,P.W. (2011) Hyaluronan as an immune regulator in human diseases. Physiol Rev. 91:221-264.

Johnston,D.J., Ramanathan,V., and McMillan,G.P. (1993) A protein from immature raspberry fruits which inhibits endopolygalacturonases from *Botrytis cinerea* and other micro-organisms. J Exp Bot 44:971-6.

Jung,S.K., Parisutham,V., Jeong,S.H., and Lee,S.K. (2012) Heterologous expression of plant cell wall degrading enzymes for

effective production of cellulosic biofuels. J.Biomed.Biotechnol. 2012:405842.

Kajava,A.V. and Kobe,B. (2002) Assessment of the ability to model proteins with leucine-rich repeats in light of the latest structural information. Protein Sci. 11:1082-1090.

Kalaitzis,P., Solomos,T., and Tucker,M.L. (1997) Three different polygalacturonases are expressed in tomato leaf and flower abscission, each with a different temporal expression pattern. Plant Physiol. 113:1303-1308.

Karabencheva,T. and Christov,C. (2010) Mechanisms of protein circular dichroism: insights from computational modeling. Adv.Protein Chem.Struct.Biol. 80:85-115.

Karimi,M., Inze,D., and Depicker,A. (2002) GATEWAY vectors for Agrobacterium-mediated plant transformation. Trends Plant Sci. 7:193-195.

Kars,I., Krooshof,G.H., Wagemakers,L., Joosten,R., Benen,J.A., and van Kan,J.A. (2005) Necrotizing activity of five *Botrytis cinerea* endopolygalacturonases produced in *Pichia pastoris*. Plant J. 43:213-225.

Kelly,S.M. and Price,N.C. (1997) The application of circular dichroism to studies of protein folding and unfolding. Biochim.Biophys.Acta 1338:161-185.

Kester,H.C.M., Kusters-van Someren,M.A., Müller,Y., and Visser,J. (1996) Primary structure and characterization of an exopolygalacturonase from *Aspergillus tubingensis*. Eur.J.Biochem. 240:738-746.

King,D., Bergmann,C., Orlando,R., Benen,J.A., Kester,H.C., and Visser,J. (2002) Use of amide exchange mass spectrometry to study conformational changes within the endopolygalacturonase II-homogalacturonan-polygalacturonase inhibiting protein system. Biochemistry 41:10225-10233.

Kobe,B. and Deisenhofer,J. (1993) Crystal structure of porcine ribonuclease inhibitor, a protein with leucine-rich repeats. Nature 366:751-756.

Kobe,B. and Kajava,A.V. (2001) The leucine-rich repeat as a protein recognition motif. Curr.Opin.Struct.Biol. 11:725-732.

Koch,M.H., Vachette,P., and Svergun,D.I. (2003) Small-angle scattering: a view on the properties, structures and structural changes

of biological macromolecules in solution. Q.Rev.Biophys. 36:147-227.

Kohorn,B.D., Kobayashi,M., Johansen,S., Friedman,H.P., Fischer,A., and Byers,N. (2006a) Wall-associated kinase 1 (WAK1) is crosslinked in endomembranes, and transport to the cell surface requires correct cell-wall synthesis. J.Cell Sci 119:2282-2290.

Kohorn,B.D., Kobayashi,M., Johansen,S., Riese,J., Huang,L.F., Koch,K., Fu,S., Dotson,A., and Byers,N. (2006b) An Arabidopsis cell wall-associated kinase required for invertase activity and cell growth. Plant J. 46:307-316.

Kratky,O., Leopold,H., and Stabinger,H. (1973) The determination of the partial specific volume of proteins by the mechanical oscillator technique. Meth.Enzymol. 27:98-110.

Krol,E., Mentzel,T., Chinchilla,D., Boller,T., Felix,G., Kemmerling,B., Postel,S., Arents,M., Jeworutzki,E., Al Rasheid,K.A., Becker,D., and Hedrich,R. (2010) Perception of the Arabidopsis danger signal peptide 1 involves the pattern recognition receptor AtPEPR1 and its close homologue AtPEPR2. J.Biol.Chem. 285:13471-13479.

Kunze,G., Zipfel,C., Robatzek,S., Niehaus,K., Boller,T., and Felix,G. (2004) The N Terminus of bacterial elongation factor Tu elicits innate immunity in Arabidopsis plants. Plant Cell 16:3496-3507.

Labat-Robert,J., Bihari-Varga,M., and Robert,L. (1990) Extracellular matrix. FEBS Lett. 268:386-393.

Lafitte,C., Barthe,J.P., Montillet,J.L., and Touzè,A. (1984) Glycoproteins inhibitors of Colletotrichum lindemuthianum endopolygalacturonase in near isogenic lines of Phaseolus vulgaris resistant and susceptible to anthracnose. Physiol Plant Pathol 25:39-53.

Lagaert,S., Belien,T., and Volckaert,G. (2009) Plant cell walls: Protecting the barrier from degradation by microbial enzymes. Semin.Cell Dev.Biol. 20:1064-1073.

Laggner,P., Glatter,O., Muller,K., Kratky,O., Kostner,G., and Holasek,A. (1977) The lipid bilayer structure of the abnormal human plasma lipoprotein X. An X-ray small-angle-scattering study. Eur.J.Biochem. 77:165-171.

Lally,D., Ingmire,P., Tong,H.Y., and He,Z.H. (2001) Antisense expression of a cell wall-associated protein kinase, WAK4, inhibits cell elongation and alters morphology. Plant Cell 13:1317-1331.

Laval,V., Chabannes,M., Carriere,M., Canut,H., Barre,A., Rouge,P., Pont-Lezica,R., and Galaud,J. (1999) A family of Arabidopsis plasma membrane receptors presenting animal beta-integrin domains. Biochim.Biophys.Acta 1435:61-70.

Leckie,F., Mattei,B., Capodicasa,C., Hemmings,A., Nuss,L., Aracri,B., De Lorenzo,G., and Cervone,F. (1999) The specificity of polygalacturonase-inhibiting protein (PGIP): a single amino acid substitution in the solvent-exposed b- strand/b-turn region of the leucine-rich repeats (LRRs) confers a new recognition capability. EMBO J. 18:2352-2363.

Leggio,C., Galantini,L., and Pavel,N.V. (2008) About the albumin structure in solution: cigar Expanded form versus heart Normal shape. Phys.Chem.Chem.Phys. 10:6741-6750.

Lipfert,J. and Doniach,S. (2007) Small-angle X-ray scattering from RNA, proteins, and protein complexes. Annu.Rev.Biophys.Biomol.Struct. 36:307-327.

Lotze,M.T., Deisseroth,A., and Rubartelli,A. (2007a) Damage associated molecular pattern molecules. Clin.Immunol. 124:1-4.

Lotze,M.T., Zeh,H.J., Rubartelli,A., Sparvero,L.J., Amoscato,A.A., Washburn,N.R., Devera,M.E., Liang,X., Tor,M., and Billiar,T. (2007b) The grateful dead: damage-associated molecular pattern molecules and reduction/oxidation regulate immunity. Immunol.Rev. 220:60-81.

Lu,D., Lin,W., Gao,X., Wu,S., Cheng,C., Avila,J., Heese,A., Devarenne,T.P., He,P., and Shan,L. (2011) Direct ubiquitination of pattern recognition receptor FLS2 attenuates plant innate immunity. Science 332:1439-1442.

Manfredini,C., Sicilia,F., Ferrari,S., Pontiggia,D., Salvi,G., Caprari,C., Lorito,M., and De Lorenzo,G. (2005) Polygalacturonase-inhibiting protein 2 of *Phaseolus vulgaris* inhibits BcPG1, a polygalacturonase of *Botrytis cinerea* important for pathogenicity, and protects transgenic plants from infection. Physiol.Mol.Plant Pathol. 67:108-115.

Marino,M., Braun,L., Cossart,P., and Ghosh,P. (1999) Structure of the lnlB leucine-rich repeats, a domain that triggers host cell invasion by the bacterial pathogen L. monocytogenes. Mol.Cell 4:1063-1072.

Marino,M., Braun,L., Cossart,P., and Ghosh,P. (2000) A framework for interpreting the leucine-rich repeats of the Listeria internalins. Proc.Natl.Acad.Sci.USA 97:8784-8788.

Mariotti,L., Casasoli,A., Caprari,C., and De Lorenzo,G. (2009) A divergent polygalacturonase of *Fusarium phyllophilum* shows sequence and functional similarity to the enzyme of *F. verticillioides*. Journal of Plant Pathology 91:129-139.

McCarty,D.R. and Chory,J. (2000) Conservation and innovation in plant signaling pathways. Cell 103:201-209.

McClendon,J.H. (1979) Subterminal polygalacturonase, a nonmacerating enzyme, attacks pectate from the reducing end. Plant Physiol 63:74-78.

McNeil,M., Darvill,A., Fry,S.C., and Albersheim,P. (1984) Structure and function of the primary cell walls of plants. Annu.Rev.Biochem. 53:625-663.

McPherson,A. and Weickmann,J. (1990) X-ray analysis of new crystal forms of the sweet protein thaumatin. J.Biomol.Struct.Dyn. 7:1053-1060.

Mertens,H.D. and Svergun,D.I. (2010) Structural characterization of proteins and complexes using small-angle X-ray solution scattering. J.Struct.Biol. 172:128-141.

Misas-Villamil,J.C. and Van der Hoorn,R.A. (2008) Enzyme-inhibitor interactions at the plant-pathogen interface. Curr.Opin.Plant Biol. 11:380-388.

Nimchuk,Z., Eulgem,T., Holt,B.F., III, and Dangl,J.L. (2003) Recognition and response in the plant immune system. Annu.Rev.Genet. 37:579-609.

Ntoukakis,V., Schwessinger,B., Segonzac,C., and Zipfel,C. (2011) Cautionary notes on the use of C-terminal BAK1 fusion proteins for functional studies. Plant Cell 23:3871-3878.

Oeser,B., Heidrich,P.M., Muller,U., Tudzynski,P., and Tenberge,K.B. (2002) Polygalacturonase is a pathogenicity factor in the *Claviceps purpurea*/rye interaction. Fungal Genet.Biol. 36:176-186.

Orthaber,D. and Glatter,O. (1998) Time and temperature dependent aggregation behaviour of the ganglioside GM1 in aqueous solution. Chem.Phys.Lipids 92:53-62.

Osakabe,Y., Yamaguchi-Shinozaki,K., Shinozaki,K., and Tran,L.S. (2013) Sensing the environment: key roles of membrane-localized kinases in plant perception and response to abiotic stress. J.Exp.Bot. 64:445-458.

Ospina-Giraldo,M.D., Mullins,E., and Kang,S. (2003) Loss of function of the *Fusarium oxysporum* SNF1 gene reduces virulence on cabbage and Arabidopsis. Curr.Genet. 44:49-57.

Otwinowski,Z. and Minor,W. (1997) Processing of X-ray Diffraction Data Collected in Oscillation Mode. In Methods in Enzymology, C.W.Carter and R.M.Sweet, eds (New York: Academic Press), pp. 307-326.

Pereira,S.F., Goss,L., and Dworkin,J. (2011) Eukaryote-like serine/threonine kinases and phosphatases in bacteria. Microbiol.Mol.Biol.Rev. 75:192-212.

Peretto,R., Favaron,F., Bettini,V., De Lorenzo,G., Marini,S., Alghisi,P., Cervone,F., and Bonfante,P. (1992) Expression and localization of polygalacturonase during the outgrowth of lateral roots in *Allium porrum* L. Planta 188:164-172.

Petoukhov,M.V., Billas,I.M., Takacs,M., Graewert,M.A., Moras,D., and Svergun,D.I. (2013) Reconstruction of quaternary structure from

X-ray scattering by equilibrium mixtures of biological macromolecules. Biochemistry 52:6844-6855.

Pickersgill,R., Smith,D., Worboys,K., and Jenkins,J. (1998) Crystal structure of polygalacturonase from Erwinia carotovora ssp. carotovora. J.Biol.Chem. 273:24660-24664.

Pilz,I., Glatter,O., and Kratky,O. (1979) Small-angle X-ray scattering. Meth.Enzymol. 61:148-249.

Pogue,G.P., Vojdani,F., Palmer,K.E., Hiatt,E., Hume,S., Phelps,J., Long,L., Bohorova,N., Kim,D., Pauly,M., Velasco,J., Whaley,K., Zeitlin,L., Garger,S.J., White,E., Bai,Y., Haydon,H., and Bratcher,B. (2010) Production of pharmaceutical-grade recombinant aprotinin and a monoclonal antibody product using plant-based transient expression systems. Plant Biotechnol.J. 8:638-654.

Poinssot,B., Vandelle,E., Bentejac,M., Adrian,M., Levis,C., Brygoo,Y., Garin,J., Sicilia,F., Coutos-Thevenot,P., and Pugin,A. (2003) The endopolygalacturonase 1 from *Botrytis cinerea* activates grapevine defense reactions unrelated to its enzymatic activity. Mol.Plant Microbe Interact. 16:553-564.

Powell,A.L.T., van Kan,J., ten Have,A., Visser,J., Greve,L.C., Bennett,A.B., and Labavitch,J.M. (2000) Transgenic expression of

pear PGIP in tomato limits fungal colonization. Mol.Plant-Microbe Interact. 13:942-950.

Raiola,A., Sella,L., Castiglioni,C., Balmas,V., and Favaron,F. (2008) A single amino acid substitution in highly similar endo-PGs from *Fusarium verticillioides* and related *Fusarium* species affects PGIP inhibition. Fungal Genet.Biol. 45:776-789.

Ranf,S., Eschen-Lippold,L., Pecher,P., Lee,J., and Scheel,D. (2011) Interplay between calcium signalling and early signalling elements during defence responses to microbe- or damage-associated molecular patterns. Plant J.

Rasul,S., Dubreuil-Maurizi,C., Lamotte,O., Koen,E., Poinssot,B., Alcaraz,G., Wendehenne,D., and Jeandroz,S. (2012) Nitric oxide production mediates oligogalacturonide-triggered immunity and resistance to *Botrytis cinerea* in *Arabidopsis thaliana*. Plant Cell Environ. 35:1483-1499.

Rexova-Benkova,L. (1973) The size of the substrate-binding site of an Aspergillus niger extracellular endopolygalacturonase. Eur.J.Biochem. 39:109-115.

Ridley,B.L., O'Neill,M.A., and Mohnen,D. (2001) Pectins: structure, biosynthesis, and oligogalacturonide-related signaling. Phytochemistry 57:929-967.

Robatzek,S., Chinchilla,D., and Boller,T. (2006) Ligand-induced endocytosis of the pattern recognition receptor FLS2 in Arabidopsis. Genes Dev. 20:537-542.

Rodriguez-Palenzuela,P., Burr,T.J., and Collmer,A. (1991) Polygalacturonase is a virulence factor in *Agrobacterium tumefaciens* biovar 3. J.Bacteriol. 173:6547-6552.

Rojo,E., Leon,J., and Sanchez-Serrano,J.J. (1999) Cross-talk between wound signalling pathways determines local versus systemic gene expression in Arabidopsis thaliana. Plant J. 20:135-142.

Royer,C.A. (2006) Probing protein folding and conformational transitions with fluorescence. Chem.Rev. 106:1769-1784.

Schilmiller,A.L. and Howe,G.A. (2005) Systemic signaling in the wound response. Curr.Opin.Plant Biol. 8:369-377.

Schubert,W.D., Urbanke,C., Ziehm,T., Beier,V., Machner,M.P., Domann,E., Wehland,J., Chakraborty,T., and Heinz,D.W. (2002) Structure of internalin, a major invasion protein of Listeria

monocytogenes, in complex with its human receptor E-cadherin. Cell 111:825-836.

Scott,P.G., McEwan,P.A., Dodd,C.M., Bergmann,E.M., Bishop,P.N., and Bella,J. (2004) Crystal structure of the dimeric protein core of decorin, the archetypal small leucine-rich repeat proteoglycan. Proc.Natl.Acad.Sci.U.S.A 101:15633-15638.

Sheludko,Y.V. (2008) Agrobacterium-mediated transient expression as an approach to production of recombinant proteins in plants. Recent Pat Biotechnol. 2:198-208.

Shiu,S.H. and Bleecker,A.B. (2001a) Plant receptor-like kinase gene family: diversity, function, and signaling. Sci.STKE. 2001:re22.

Shiu,S.H. and Bleecker,A.B. (2001b) Receptor-like kinases from Arabidopsis form a monophyletic gene family related to animal receptor kinases. Proc.Natl.Acad.Sci.USA 98:10763-10768.

Shiu,S.H. and Bleecker,A.B. (2003) Expansion of the receptor-like kinase/Pelle gene family and receptor-like proteins in Arabidopsis. Plant Physiol 132:530-543.

Sicilia,F., Fernandez-Recio,J., Caprari,C., De Lorenzo,G., Tsernoglou,D., Cervone,F., and Federici,L. (2005) The polygalacturonase-inhibiting protein PGIP2 of *Phaseolus vulgaris*

has evolved a mixed mode of inhibition of endopolygalacturonase PG1 of *Botrytis cinerea*. Plant Physiol. 139:1380-1388.

Sikder,A.R. and Zomaya,A.Y. (2005) An overview of protein-folding techniques: issues and perspectives. Int.J.Bioinform.Res.Appl. 1:121-143.

Sivaguru,M., Ezaki,B., He,Z.H., Tong,H.Y., Osawa,H., Baluska,F., Volkmann,D., and Matsumoto,H. (2003) Aluminum-induced gene expression and protein localization of a cell wall-associated receptor kinase in Arabidopsis. Plant Physiol. 132:2256-2266.

Smith,J.M., Salamango,D.J., Leslie,M.E., Collins,C.A., and Heese,A. (2013) Sensitivity to flg22 is modulated by ligand-induced degradation and de novo synthesis of the endogenous flagellin-receptor FLS2. Plant Physiol.

Somerville,C., Bauer,S., Brininstool,G., Facette,M., Hamann,T., Milne,J., Osborne,E., Paredez,A., Persson,S., Raab,T., Vorwerk,S., and Youngs,H. (2004) Toward a systems approach to understanding plant cell walls. Science 306:2206-2211.

Spinelli, F., Mariotti, L., Mattei, B., Salvi, G., Cervone, F., and Caprari, C. Three aspartic acid residues of polygalacturonase

inhibiting protein (PGIP) from *Phaseolus vulgaris* are critical for inhibition of *Fusarium phyllophilum* PG. Plant Biology . 2009.
Ref Type: In Press

Stotz,H.U., Bishop,J.G., Bergmann,C.W., Koch,M., Albersheim,P., Darvill,A.G., and Labavitch,J.M. (2000) Identification of target amino acids that effect interactions of fungal polygalacturonases and their plant inhibitors. Physiol.Mol.Plant Pathol. 56:117-130.

Stumpp,M.T., Forrer,P., Binz,H.K., and Pluckthun,A. (2003) Designing repeat proteins: modular leucine-rich repeat protein libraries based on the mammalian ribonuclease inhibitor family. J.Mol.Biol. 332:471-487.

Sutherland,B.W., Toews,J., and Kast,J. (2008) Utility of formaldehyde cross-linking and mass spectrometry in the study of protein-protein interactions. J.Mass Spectrom. 43:699-715.

Svergun,D.I. (1999) Restoring low resolution structure of biological macromolecules from solution scattering using simulated annealing. Biophys.J. 76:2879-2886.

Svergun,D.I. (2010) Small-angle X-ray and neutron scattering as a tool for structural systems biology. Biol.Chem. 391:737-743.

Svergun,D.I., Petoukhov,M.V., and Koch,M.H. (2001) Determination of domain structure of proteins from X-ray solution scattering. Biophys.J. 80:2946-2953.

Tabarani,G., Thepaut,M., Stroebel,D., Ebel,C., Vives,C., Vachette,P., Durand,D., and Fieschi,F. (2009) DC-SIGN neck domain is a pH-sensor controlling oligomerization: SAXS and hydrodynamic studies of extracellular domain. J.Biol.Chem. 284:21229-21240.

ten Have,A., Mulder,W., Visser,J., and van Kan,J.A. (1998) The endopolygalacturonase gene *Bcpg1* is required for full virulence of *Botrytis cinerea*. Mol Plant Microbe Interact. 11:1009-16.

Torki,M., Mandaron,P., Thomas,F., Quigley,F., Mache,R., and Falconet,D. (1999) Differential expression of a polygalacturonase gene family in *Arabidopsis thaliana*. Mol.Gen.Genet. 261:948-952.

Torres,M.A., Jones,J.D., and Dangl,J.L. (2006a) Reactive oxygen species signaling in response to pathogens. Plant Physiol 141:373-378.

Torres,M.A., Jones,J.D., and Dangl,J.L. (2006b) Reactive oxygen species signaling in response to pathogens. Plant Physiol. 141:373-378.

Vagin,A. and Teplyakov,A. (2000) An approach to multi-copy search in molecular replacement. Acta Crystallogr.D.Biol.Crystallogr. 56:1622-1624.

van Santen,Y., Benen,J.A., Schroter,K.H., Kalk,K.H., Armand,S., Visser,J., and Dijkstra,B.W. (1999) 1.68-A crystal structure of endopolygalacturonase II from *Aspergillus niger* and identification of active site residues by site-directed mutagenesis. J.Biol.Chem. 274:30474-30480.

Vasilescu,J., Guo,X., and Kast,J. (2004) Identification of protein-protein interactions using in vivo cross-linking and mass spectrometry. Proteomics 4:3845-3854.

Verica,J.A., Chae,L., Tong,H.Y., Ingmire,P., and He,Z.H. (2003) Tissue-specific and developmentally regulated expression of a cluster of tandemly arrayed cell wall-associated kinase-like kinase genes in Arabidopsis. Plant Physiol. 133:1732-1746.

Wagner,T.A. and Kohorn,B.D. (2001) Wall-Associated kinases are expressed throughout plant development and are required for cell expansion. Plant Cell 13:303-318.

Walker,J.C. (1994) Structure and function of the receptor-like protein kinases of higher plants. Plant Mol.Biol. 26:1599-1609.

Wang,Z.Y., MacRae,E.A., Wright,M.A., Bolitho,K.M., Ross,G.S., and Atkinson,R.G. (2000) Polygalacturonase gene expression in kiwifruit: relationship to fruit softening and ethylene production. Plant Mol.Biol. 42:317-328.

Willats,W.G., Limberg,G., Buchholt,H.C., van Alebeek,G.J., Benen,J., Christensen,T.M., Visser,J., Voragen,A., Mikkelsen,J.D., and Knox,J.P. (2000) Analysis of pectic epitopes recognised by hybridoma and phage display monoclonal antibodies using defined oligosaccharides, polysaccharides, and enzymatic degradation [In Process Citation]. Carbohydr.Res. 327:309-320.

YANARI,S. and BOVEY,F.A. (1960) Interpretation of the ultraviolet spectral changes of proteins. J.Biol.Chem. 235:2818-2826.

Yoder,M.D., Keen,N.T., and Jurnak,F. (1993) New domain motif: The structure of pectate lyase C, a secreted plant virulence factor. Science 260:1503-1507.

Zhang,S., Chen,C., Li,L., Meng,L., Singh,J., Jiang,N., Deng,X.W., He,Z.H., and Lemaux,P.G. (2005) Evolutionary expansion, gene structure, and expression of the rice wall-associated kinase gene family. Plant Physiol 139:1107-1124.

Zhang,X., Dai,Y., Xiong,Y., DeFraia,C., Li,J., Dong,X., and Mou,Z. (2007) Overexpression of Arabidopsis MAP kinase kinase 7 leads to activation of plant basal and systemic acquired resistance. Plant J. 52:1066-1079.

Zhang,Y., Cao,L., Yang,B.L., and Yang,B.B. (1998) The G3 domain of versican enhances cell proliferation via epidermial growth factor-like motifs. J.Biol.Chem. 273:21342-21351.

Zipfel,C. (2009) Early molecular events in PAMP-triggered immunity. Curr.Opin.Plant Biol. 12:414-420.

Zipfel,C., Kunze,G., Chinchilla,D., Caniard,A., Jones,J.D.G., Boller,T., and Felix,G. (2006) Perception of the bacterial PAMP EF-Tu by the receptor EFR restricts *Agrobacterium*-mediated transformation. Cell 125:749-760.

Zuppini,A., Navazio,L., Sella,L., Castiglioni,J., Favaron,F., and Mariani,P. (2005) An endopolygalacturonase from *Sclerotinia sclerotiorum* induces calcium-mediated signaling and programmed cell death in soybean cells. Mol.Plant Microbe Interact. 18:849-855.

Ringraziamenti

Il capitolo più semplice da scrivere su di una tesi dovrebbero essere i ringraziamenti; non è così per me. Ho trovato sempre una, pur se minima, difficoltà nella stesura di questo capitolo; scrivere questo, poi, è molto difficile, qui si chiude un'era, un periodo, un viaggio.
Vorrei ringraziare *in primis* il Prof. Cervone, che mi ha permesso di proseguire, dopo la laurea Magistrale, questo lungo cammino nel mondo del Dottorato. Ringrazio la Prof. ssa De Lorenzo per la sua sempre vivida attenzione alle problematiche della mia ricerca, aiutandomi quando ne avevo bisogno.
Senza alcune persone tutto questo non sarebbe potuto accadere: vorrei infatti ringraziare Manuel, che mi ha supportato e sopportato in questi anni, senza battere ciglio o arrendersi mai. Ringrazio Francesco, Sara e Lucia (M) per le lunghe giornate passate in laboratorio, mentre fra una sigaretta e l'altra provavamo a fare Scienza. Ringrazio le mie due compagne di Dottorato, Giovanna e Vanessa, con le quali ho condiviso tutti gli aspetti di questo percorso, da quelli burocratici a quelli più gioviali. Ringrazio Francesca per avermi fornito le basi per riuscire a cavarmela da solo in questi anni. Ringrazio Ilaria, Damiano, Nora, Daniel e Matteo, per tutto il tempo che abbiamo passato insieme, sempre. A questo punto è doveroso ringraziare mio padre, mia madre e mio fratello, che mi sono stati sempre accanto e senza i quali tutto questo non sarebbe mai accaduto. Infine ringrazio Marco per esser stato il motore delle nostre lunghe ed infinite chiacchierate che mi hanno spronato ad andare sempre avanti senza arrendersi mai.